Optimization methods in direct and inverse scattering

Alexander G. RAMM and Semion GUTMAN

Abstract. In many Direct and Inverse Scattering problems one has to use a parameter-fitting procedure, because analytical inversion procedures are often not available. In this paper a variety of such methods is presented with a discussion of theoretical and computational issues.

The problem of finding small subsurface inclusions from surface scattering data is stated and investigated. This Inverse Scattering problem is reduced to an optimization problem, and solved by the Hybrid Stochastic-Deterministic minimization algorithm. A similar approach is used to determine layers in a particle from the scattering data.

The Inverse potential scattering problem is described and its solution based on a parameter fitting procedure is presented for the case of spherically symmetric potentials and fixed-energy phase shifts as the scattering data. The central feature of the minimization algorithm here is the Stability Index Method. This general approach estimates the size of the minimizing sets, and gives a practically useful stopping criterion for global minimization algorithms.

The 3D inverse scattering problem with fixed-energy data is discussed. Its solution by the Ramm's method is described. The cases of exact and noisy discrete data are considered. Error estimates for the inversion algorithm are given in both cases of exact and noisy data. Comparison of the Ramm's inversion method with the inversion based on the Dirichlet-to-Neumann map is given and it is shown that there are many more numerical difficulties in the latter method than in the Ramm's method.

An Obstacle Direct Scattering problem is treated by a novel Modified Rayleigh Conjecture (MRC) method. MRC's performance is compared favorably to the well known Boundary Integral Equation Method, based on the properties of the single and double-layer potentials. A special minimization procedure allows one to inexpensively compute scattered fields for 2D and 3D obstacles having smooth as well as nonsmooth surfaces.

A new Support Function Method (SFM) is used for Inverse Obstacle Scattering problems. The SFM can work with limited data. It can also be used for Inverse scattering problems with *unknown scattering conditions on its boundary (e.g. soft, or hard scattering)*. Another method for Inverse scattering problems, the Linear Sampling Method (LSM), is analyzed. Theoretical and computational difficulties in using this method are pointed out.

Key words and phrases: inverse and direct scattering, optimization, Modified Rayleigh Conjecture, support function method, stability index, Ramm's method, small inhomogeneities, linear sampling method.

1991 *Mathematics Subject Classification.* Primary 78A46, 65N21, Secondary 35R30.

Contents

1. Introduction.

Suppose that an acoustic or electromagnetic wave encounters an inhomogeneity and, as a consequence, gets scattered. The problem of finding the scattered wave assuming the knowledge of the inhomogeneity (penetrable or not) is the Direct Scattering problem. An impenetrable inhomogeneity is also called an obstacle. On the other hand, if the scattered wave is known at some points outside an inhomogeneity, then we are faced with the Inverse Scattering problem, the goal of which is to identify this inhomogeneity, see [**50, 55, 56, 17, 16**]

Among a variety of methods available to handle such problems few provide a mathematically justified algorithm. In many cases one has to use a parameter-fitting procedure, especially for inverse scattering problems, because the analytical inversion procedures are often not available. An important part of such a procedure is an efficient global optimization method, see [**24, 25, 35, 36, 45, 82**].

The general scheme for parameter-fitting procedures is simple: one has a relation $B(q) = A$, where B is some operator, q is an unknown function, and A is the data. In inverse scattering problems q is an unknown potential, and A is the known scattering amplitude. If q is sought in a finite-parametric family of functions, then $q = q(x, p)$, where $p = (p_1, ..., p_n)$ is a parameter. The parameter is found by solving a global minimization problem: $\Phi[B(q(x, p)) - A] = \min$, where Φ is some positive functional, and $q \in Q$, where Q is an admissible set of q. In practice the above problem often has many local minimizers, and the global minimizer is not necessarily unique. In [**55**] and [**57**] some functionals Φ are constructed which have unique global minimizer, namely, the solution to inverse scattering problem, and the global minimum is zero.

Moreover, as a rule, the data A is known with some error. Thus A_δ is known, such that $||A - A_\delta|| < \delta$. There are no stability estimates which would show how the global minimizer $q(x, p_{opt})$ is perturbed when the data A are replaced by the perturbed data A_δ. In fact, one can easily construct examples showing that there is no stability of the global minimizer with respect to small errors in the data, in general.

For these reasons there is no guarantee that the parameter-fitting procedures would yield a solution to the inverse problem with a guaranteed accuracy. However, overwhelming majority of practitioners are using parameter-fitting procedures. In dozens of published papers the results obtained by various parameter-fitting procedures look quite good. The explanation, in most of the cases is simple: the

authors know the answer beforehand, and it is usually not difficult to parametrize the unknown function so that the exact solution is well approximated by a function from a finite-parametric family, and since the authors know a priori the exact answer, they may choose numerically the values of the parameters which yield a good approximation of the exact solution. *When can one rely on the results obtained by parameter-fitting procedures? Unfortunately, there is no rigorous and complete answer to this question, but some recommendations are given in Section 4.*

In this paper the authors present their recent results which are based on specially designed parameter-fitting procedures. Before describing them, let us mention that usually in a numerical solution of an inverse scattering problem one uses a regularization procedure, e.g. a variational regularization, spectral cut-off, iterative regularization, DSM (the dynamical systems method), quasi-solutions, etc, see e.g. [**78**], [**73**]. This general theoretical framework is well established in the theory of ill-posed problems, of which the inverse scattering problems represent an important class. This framework is needed to achieve a stable method for assigning a solution to an ill-posed problem, usually set in an infinite dimensional space. The goal of this paper is to present optimization algorithms already in a finite dimensional setting of a Direct or Inverse scattering problem.

In Section 2 the problem of finding small subsurface inclusions from surface scattering data is investigated ([**61**]). This (geophysical) Inverse Scattering problem is reduced to an optimization problem. This problem is solved by the Hybrid Stochastic-Deterministic minimization algorithm ([**27**]). It is based on a genetic minimization algorithm ideas for its random (stochastic) part, and a deterministic minimization without derivatives used for the local minimization part.

In Section 3 a similar approach is used to determine layers in a particle subjected to acoustic or electromagnetic waves. The global minimization algorithm uses Rinnooy Kan and Timmer's Multilevel Single-Linkage Method for its stochastic part.

In Section 4 we discuss an Inverse potential scattering problem appearing in a quantum mechanical description of particle scattering experiments. The central feature of the minimization algorithm here is the Stability Index Method ([**72**]). This general approach estimates the size of the minimizing sets, and gives a practically useful stopping criterion for global minimization algorithms.

In Section 5 Ramm's method for solving 3D inverse scattering problem with fixed-energy data is presented following [**79**], see also [**68**]. The cases of exact and noisy discrete data are considered. Error estimates for the inversion algorithm are given in both cases of exact and noisy data. Comparison of the Ramm's inversion method with the inversion based on the Dirichlet-to-Neumann map is given and it is shown that there are many more numerical difficulties in the latter method than in Ramm's method.

In Section 6 an Obstacle Direct Scattering problem is treated by a novel Modified Rayleigh Conjecture (MRC) method. It was introduced in [**69**] and applied in [**30, 32**] and [**75**]. MRC's performance is compared favorably to the well known Boundary Integral Equation Method, based on the properties of the single and double-layer potentials. A special minimization procedure allows us to inexpensivly compute scattered fields for several 2D and 3D obstacles having smooth as well as nonsmooth surfaces.

In Section 7 a new Support Function Method (SFM) is used to determine the location of an obstacle (cf [**48**], [**50**], [**31**]). Unlike other methods, the SFM can work with limited data. It can also be used for Inverse scattering problems with *unknown scattering conditions on its boundary (e.g. soft, or hard scattering).*

Finally, in Section 8, we present an analysis of another popular method for Inverse scattering problems, the Linear Sampling Method (LSM), and show that both theoretically and computationally the method fails in many aspects.

2. Identification of small subsurface inclusions.

2.1. Problem description. In many applications it is desirable to find small inhomogeneities from surface scattering data. For example, such a problem arises in ultrasound mammography, where small inhomogeneities are cancer cells. Other examples include the problem of finding small holes and cracks in metals and other materials, or the mine detection. The scattering theory for small scatterers originated in the classical works of Lord Rayleigh (1871). Rayleigh understood that the basic contribution to the scattered field in the far-field zone comes from the dipole radiation, but did not give methods for calculating this radiation. Analytical formulas for calculating the polarizability tensors for homogeneous bodies of arbitrary shapes were derived in [**50**] (see also references therein). These formulas allow one to calculate the S-matrix for scattering of acoustic and electromagnetic waves by small bodies of arbitrary shapes with arbitrary accuracy. Inverse scattering problems for small bodies are considered in [**49**] and [**56**]. In [**61**] the problem of identification of small subsurface inhomogeneities from surface data was posed and its possible applications were discussed.

In the context of a geophysical problem, let $y \in \mathbb{R}^3$ be a point source of monochromatic acoustic waves on the surface of the earth. Let $u(x, y, k)$ be the acoustic pressure at a point $x \in \mathbb{R}^3$, and $k > 0$ be the wavenumber. The governing equation for the acoustic wave propagation is:

$$\left[\nabla^2 + k^2 + k^2 v(x)\right] u = -\delta(x - y) \text{ in } \mathbb{R}^3, \tag{2.1}$$

where $x = (x_1, x_2, x_3)$, $v(x)$ is the inhomogeneity in the velocity profile, and $u(x, y, k)$ satisfies the radiation condition at infinity, i.e. it decays sufficiently fast as $|x| \to \infty$.

Let us assume that $v(x)$ is a bounded function vanishing outside of the domain $D = \cup_{m=1}^{M} D_m$ which is the union of M small nonintersecting domains D_m, all of them are located in the lower half-space $\mathbb{R}^3_- = \{x : x_3 < 0\}$. Smallness is understood in the sense $k\rho \ll 1$, where $\rho := \frac{1}{2}\max_{1\le m\le M}\{\operatorname{diam} D_m\}$, and diam D is the diameter of the domain D. Practically $k\rho \ll 1$ means that $k\rho < 0.1$. In some cases $k\rho < 0.2$ is sufficient for obtaining acceptable numerical results. The background velocity in (2.1) equals to 1, but we can consider the case of fairly general background velocity [**56**].

Denote $\tilde{z}_m$ and $\tilde{v}_m$ the position of the center of gravity of D_m, and the total intensity of the m-th inhomogeneity $\tilde{v}_m := \int_{D_m} v(x)dx$. Assume that $\tilde{v}_m \neq 0$. Let P be the equation of the surface of the earth:

$$P := \{x = (x_1, x_2, x_3) \in \mathbb{R}^3 : x_3 = 0\}. \tag{2.2}$$

The inverse problem to be solved is:

IP: *Given $u(x, y, k)$ for all source-detector pairs (x, y) on P at a fixed $k > 0$, find the number M of small inhomogeneities, the positions $\tilde{z}_m$ of the inhomogeneities, and their intensities $\tilde{v}_m$.*

Practically, one assumes that a fixed wavenumber $k > 0$, and J source-detector pairs $(x_j, y_j), j = 1, 2, ..., J$, on P are known together with the acoustic pressure measurements $u(x_j, y_j, k)$. Let

$$g(x, y, k) := \frac{\exp(ik|x - y|)}{4\pi|x - y|}, \quad x, y \in P, \tag{2.3}$$

$$G_j(z) := G(x_j, y_j, z) := g(x_j, z, k)g(y_j, z, k), \quad x_j, y_j \in P,\ z \in \mathbb{R}^3_-, \tag{2.4}$$

$$f_j := \frac{u(x_j, y_j, k) - g(x_j, y_j, k)}{k^2}, \tag{2.5}$$

and

$$\Phi(z_1, \ldots, z_M,\, v_1, \ldots, v_M) := \sum_{j=1}^{J} \left| f_j - \sum_{m=1}^{M} G_j(z_m) v_m \right|^2 . \tag{2.6}$$

The proposed method for solving the (IP) consists of finding the global minimizer of function (2.6). This minimizer $(\tilde{z}_1, \ldots, \tilde{z}_M,\, \tilde{v}_1, \ldots, \tilde{v}_M)$ gives the estimates of the positions $\tilde{z}_m$ of the small inhomogeneities and their intensities $\tilde{v}_m$. See [**61**] for a justification of this approach.

The function Φ depends on M unknown points $z_m \in \mathbb{R}^3_-$, and M unknown parameters v_m, $1 \le m \le M$. The number M of the small inhomogeneities is also unknown, and its determination is a part of the minimization problem.

2.2. Hybrid Stochastic-Deterministic Method. Let the inhomogeneities be located within the box

$$B = \{(x_1, x_2, x_3)\ : -a < x_1 < a,\ -b < x_2 < b,\ 0 < x_3 < c\}\,, \tag{2.7}$$

and their intensities satisfy

$$0 \le v_m \le v_{max}\,. \tag{2.8}$$

The box is located above the earth surface for a computational convenience.

Then, given the location of the points $z_1, z_2, \ldots, z_M$, the minimum of Φ with respect to the intensities $v_1, v_2, \ldots, v_M$ can be found by minimizing the resulting quadratic function in (2.6) over the region satisfying (2.8). This can be done using normal equations for (2.6) and projecting the resulting point back onto the region defined by (2.8). Denote the result of this minimization by $\tilde{\Phi}$, that is

$$\begin{aligned} \tilde{\Phi}(z_1, z_2, \ldots, z_M) = \min\{&\Phi(z_1, z_2, \ldots, z_M, v_1, v_2, \ldots, v_M)\ : \\ &0 \le v_m \le v_{max}\,, \quad 1 \le m \le M\} \end{aligned} \tag{2.9}$$

Now the original minimization problem for $\Phi(z_1, z_2, \ldots, z_M, v_1, v_2, \ldots, v_M)$ is reduced to the $3M$-dimensional constrained minimization for $\tilde{\Phi}(z_1, z_2, \ldots, z_M)$:

$$\tilde{\Phi}(z_1, z_2, \ldots, z_M) = \min\,, \quad z_m \in B\,, \quad 1 \le m \le M\,. \tag{2.10}$$

Note, that the dependency of $\tilde{\Phi}$ on its $3M$ variables (the coordinates of the points z_m) is highly nonlinear. In particular, this dependency is complicated by

the computation of the minimum in (2.9) and the consequent projection onto the admissible set B. Thus, an analytical computation of the gradient of $\tilde{\Phi}$ is not computationally efficient. Accordingly, the Powell's quadratic minimization method was used to find local minima. This method uses a special procedure to numerically approximate the gradient, and it can be shown to exhibit the same type of quadratic convergence as conjugate gradient type methods (see [**11**]).

In addition, *the exact number of the original inhomogeneities M_{orig} is unknown, and its estimate is a part of the inverse problem.* In the HSD algorithm described below this task is accomplished by taking the initial number M sufficiently large, so that

$$M_{orig} \leq M\,, \tag{2.11}$$

which, presumably, can be estimated from physical considerations. After all, our goal is to find only the strongest inclusions, since the weak ones cannot be distinguished from background noise. The Reduction Procedure (see below) allows the algorithm to seek the minimum of $\tilde{\Phi}$ in a lower dimensional subsets of the admissible set B, thus finding the estimated number of inclusions M. Still another difficulty in the minimization is a large number of local minima of $\tilde{\Phi}$. This phenomenon is well known for objective functions arising in various inverse problems, and we illustrate this point in Figure 1.

For example, let $M_{orig} = 6$, and the coordinates of the inclusions, and their intensities $(\tilde{z}_1, \dots, \tilde{z}_6, \tilde{v}_1, \dots, \tilde{v}_6)$ be as in Table 1. Figure 1 shows the values of the function $\tilde{\Phi}(z_r, z_2, \tilde{z}_3, \tilde{z}_4, \tilde{z}_5, \tilde{z}_6)$, where

$$z_r = (r, 0, 0.520)\,, \quad -2 \leq r \leq 2$$

and

$$z_2 = (-1, 0.3, 0.580)\,.$$

The plot shows multiple local minima and almost flat regions.

A direct application of a gradient type method to such a function would result in finding a local minimum, which may or may not be the sought global one. In the example above, such a method would usually be trapped in a local minimum located at $r = -2$, $r = -1.4$, $r = -0.6$, $r = 0.2$ or $r = 0.9$, and the desired global minimum at $r = 1.6$ would be found only for a sufficiently close initial guess $1.4 < r < 1.9$. Various global minimization methods are known (see below), but we found that an efficient way to accomplish the minimization task for this Inverse Problem was to design a new method (HSD) combining both the stochastic and the deterministic approach to the global minimization. Deterministic minimization algorithms with or without the gradient computation, such as the conjugate gradient methods, are known to be efficient (see [**11, 20, 46, 38**]), and [**82**]. However, the initial guess should be chosen sufficiently close to the sought minimum. Also such algorithms tend to be trapped at a local minimum, which is not necessarily close to a global one. A new deterministic method is proposed in [**5**] and [**6**], which is quite efficient according to [**6**]. On the other hand, various stochastic minimization algorithms, e.g. the simulated annealing method [**39, 40**], are more likely to find a global minimum, but their convergence can be very slow. We have tried a variety of minimization algorithms to find an acceptable minimum of $\tilde{\Phi}$. Among them were the Levenberg-Marquardt Method, Conjugate Gradients, Downhill Simplex, and Simulated Annealing Method. None of them produced consistent satisfactory results.

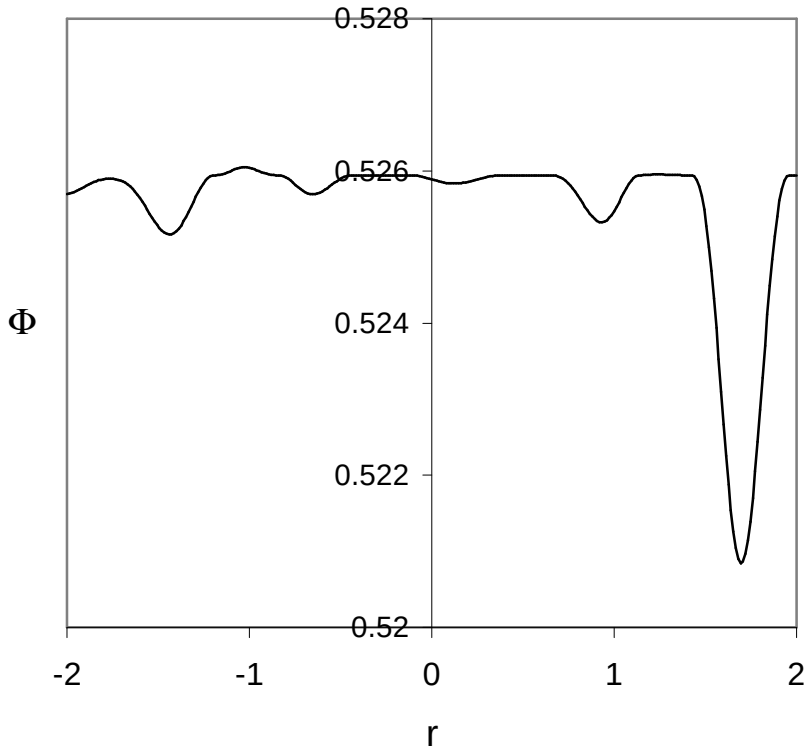

FIGURE 1. Objective function $\tilde{\Phi}(z_r, z_2, \tilde{z}_3, \tilde{z}_4, \tilde{z}_5, \tilde{z}_6)\,, \quad -2 \le r \le 2$

Among minimization methods combining random and deterministic searches we mention Deep's method [**19**] and a variety of clustering methods [**80**], [**81**]. An application of these methods to the particle identification using light scattering is described in [**84**]. The clustering methods are quite robust (that is, they consistently find global extrema) but, usually, require a significant computational effort. One such method is described in the next section on the identification of layers in a multilayer particle. The HSD method is a combination of a reduced sample random search method with certain ideas from Genetic Algorithms (see e.g. [**33**]). It is very efficient and seems especially well suited for low dimensional global minimization. Further research is envisioned to study its properties in more detail, and its applicability to other problems.

The steps of the Hybrid Stochastic-Deterministic (HSD) method are outlined below. Let us call a collection of M points (inclusion's centers) $\{z_1, z_2, ..., z_M\},\ z_i \in B$ a *configuration* Z. Then the minimization problem (2.10) is the minimization of the objective function $\tilde{\Phi}$ over the set of all configurations.

For clarity, let $P_0 = 1,\ \epsilon_s = 0.5,\ \epsilon_i = 0.25,\ \epsilon_d = 0.1$, be the same values as the ones used in numerical computations in the next section.

Generate a random configuration Z. Compute the best fit intensities v_i corresponding to this configuration. If $v_i > v_{max}$, then let $v_i := v_{max}$. If $v_i < 0$, then let $v_i := 0$. If $\tilde{\Phi}(Z) < P_0\epsilon_s$, then this configuration is a preliminary candidate for the initial guess of a deterministic minimization method (Step 1).

Drop the points $z_i \in Z$ such that $v_i < v_{max}\epsilon_i$. That is, the inclusions with small intensities are eliminated (Step 2).

If two points $z_k, z_j \in Z$ are too close to each other, then replace them with one point of a combined intensity (Step 3).

After completing steps 2 and 3 we would be left with $N \leq M$ points $z_1, z_2, ..., z_N$ (after a re-indexing) of the original configuration Z. Use this reduced configuration Z_{red} as the starting point for the deterministic restraint minimization in the $3N$ dimensional space (Step 4). Let the resulting minimizer be $\tilde{Z}_{red} = (\tilde{z}_1, ..., \tilde{z}_N)$. If the value of the objective function $\tilde{\Phi}(\tilde{Z}_{red}) < \epsilon$, then we are done: $\tilde{Z}_{red}$ is the sought configuration containing N inclusions. If $\tilde{\Phi}(\tilde{Z}_{red}) \geq \epsilon$, then the iterations should continue.

To continue the iteration, randomly generate $M - N$ points in B (Step 5). Add them to the reduced configuration $\tilde{Z}_{red}$. Now we have a new full configuration Z, and the iteration process can continue (Step 1).

This entire iterative process is repeated n_{max} times, and the best configuration is declared to represent the sought inclusions.

2.3. Hybrid Stochastic-Deterministic (HSD) Method. Let P_0, T_{max}, n_{max}, ϵ_s, ϵ_i, ϵ_d, and ϵ be positive numbers. Let a positive integer M be larger than the expected number of inclusions. Let $N = 0$.

(1) Randomly generate $M - N$ additional points $z_{N+1}, \ldots, z_M \in B$ to obtain a full configuration $Z = (z_1, \ldots, z_M)$. Find the best fit intensities v_i, $i = 1, 2, ..., M$. If $v_i > v_{max}$, then let $v_i := v_{max}$. If $v_i < 0$, then let $v_i := 0$. Compute $P_s = \tilde{\Phi}(z_1, z_2 \ldots, z_M)$. If $P_s < P_0\epsilon_s$ then go to step 2, otherwise repeat step 1.
(2) Drop all the points with the intensities v_i satisfying $v_i < v_{max}\epsilon_i$. Now only $N \leq M$ points $z_1, z_2 \ldots, z_N$ (re-indexed) remain in the configuration Z.
(3) If any two points z_m, z_n in the above configuration satisfy $|z_m - z_n| < \epsilon_d D$, where $D = diam(B)$, then eliminate point z_n, change the intensity of point z_m to $v_m + v_n$, and assign $N := N - 1$. This step is repeated until no further reduction in N is possible. Call the resulting reduced configuration with N points by Z_{red}.
(4) Run a constrained deterministic minimization of $\tilde{\Phi}$ in $3N$ variables, with the initial guess Z_{red}. Let the minimizer be $\tilde{Z}_{red} = (\tilde{z}_1, \ldots, \tilde{z}_N)$. If $P = \tilde{\Phi}(\tilde{z}_1, \ldots, \tilde{z}_N) < \epsilon$, then save this configuration, and go to step 6, otherwise let $P_0 = P$, and proceed to the next step 5.
(5) Keep intact N points $\tilde{z}_1, \ldots, \tilde{z}_N$. If the number of random configurations has exceeded T_{max} (the maximum number of random tries), then save the configuration and go to step 6, otherwise go to step 1, and use these N points there.
(6) Repeat steps 1 through 5 n_{max} times.
(7) Find the configuration among the above n_{max} ones, which gives the smallest value to $\tilde{\Phi}$. This is the best fit.

TABLE 1. Actual inclusions.

Inclusions	x_1	x_2	x_3	v
1	1.640	-0.510	0.520	1.200
2	-1.430	-0.500	0.580	0.500
3	1.220	0.570	0.370	0.700
4	1.410	0.230	0.740	0.610
5	-0.220	0.470	0.270	0.700
6	-1.410	0.230	0.174	0.600

The Powell's minimization method (see [**11**] for a detailed description) was used for the deterministic part, since this method does not need gradient computations, and it converges quadratically near quadratically shaped minima. Also, in step 1, an idea from the Genetic Algorithm's approach [**33**] is implemented by keeping only the strongest representatives of the population, and allowing a mutation for the rest.

2.4. Numerical results. The algorithm was tested on a variety of configurations. Here we present the results of just two typical numerical experiments illustrating the performance of the method. In both experiments the box B is taken to be

$$B = \{(x_1, x_2, x_3) \ : -a < x_1 < a, \ -b < x_2 < b, \ 0 < x_3 < c\},$$

with $a = 2, \ b = 1, \ c = 1$. The wavenumber $k = 5$, and the effective intensities v_m are in the range from 0 to 2. The values of the parameters were chosen as follows

$$P_0 = 1\,, T_{max} = 1000,\, \epsilon_s = 0.5,\, \epsilon_i = 0.25,\, \epsilon_d = 0.1\,, \epsilon = 10^{-5}\,, n_{max} = 6$$

In both cases we searched for the same 6 inhomogeneities with the coordinates x_1, x_2, x_3 and the intensities v shown in Table 1.

Parameter M was set to 16, thus the only information on the number of inhomogeneities given to the algorithm was that their number does not exceed 16. This number was chosen to keep the computational time within reasonable limits. Still another consideration for the number M is the aim of the algorithm to find the presence of the most influential inclusions, rather then all inclusions, which is usually impossible in the presence of noise and with the limited amount of data.

Experiment 1. In this case we used 12 sources and 21 detectors, all on the surface $x_3 = 0$. The sources were positioned at $\{(-1.667{+}0.667i, -0.5{+}1.0j, 0),\ i = 0, 1, \ldots, 5,\ j = 0, 1\}$, that is 6 each along two lines $x_2 = -0.5$ and $x_2 = 0.5$. The detectors were positioned at $\{(-2 + 0.667i, -1.0 + 1.0j, 0),\ i = 0, 1, \ldots, 6,\ j = 0, 1, 2\}$, that is seven detectors along each of the three lines $x_2 = -1$, $x_2 = 0$ and $x_2 = 1$. This corresponds to a mammography search, where the detectors and the sources are placed above the search area. The results for noise level $\delta = 0.00$ are shown in Figure 2 and Table 2. The results for noise level $\delta = 0.05$ are shown in Table 3.

Experiment 2. In this case we used 8 sources and 22 detectors, all on the surface $x_3 = 0$. The sources were positioned at $\{(-1.75 + 0.5i, 1.5, 0),\ i = 0, 1, \ldots, 7,\ j = 0, 1\}$, that is all 8 along the line $x_2 = 1.5$. The detectors were positioned at $\{(-2 + 0.4i, 1.0 + 1.0j, 0),\ i = 0, 1, \ldots, 10,\ j = 0, 1\}$, that is eleven detectors along each of the two lines $x_2 = 1$ and $x_2 = 2$. This corresponds to a mine

TABLE 2. Experiment 1. Identified inclusions, no noise, $\delta = 0.00$.

x_1	x_2	x_3	v
1.640	-0.510	0.520	1.20000
-1.430	-0.500	0.580	0.50000
1.220	0.570	0.370	0.70000
1.410	0.230	0.740	0.61000
-0.220	0.470	0.270	0.70000
-1.410	0.230	0.174	0.60000

TABLE 3. Experiment 1. Identified inclusions, $\delta = 0.05$.

x_1	x_2	x_3	v
1.645	-0.507	0.525	1.24243
1.215	0.609	0.376	0.67626
-0.216	0.465	0.275	0.69180
-1.395	0.248	0.177	0.60747

TABLE 4. Experiment 2. Identified inclusions, no noise, $\delta = 0.00$.

x_1	x_2	x_3	v
1.656	-0.409	0.857	1.75451
-1.476	-0.475	0.620	0.48823
1.209	0.605	0.382	0.60886
-0.225	0.469	0.266	0.69805
-1.406	0.228	0.159	0.59372

TABLE 5. Experiment 2. Identified inclusions, $\delta = 0.05$.

x_1	x_2	x_3	v
1.575	-0.523	0.735	1.40827
-1.628	-0.447	0.229	1.46256
1.197	0.785	0.578	0.53266
-0.221	0.460	0.231	0.67803

search, where the detectors and the sources must be placed outside of the searched ground. The results of the identification for noise level $\delta = 0.00$ in the data are shown in Figure 3 and Table 4. The results for noise level $\delta = 0.05$ are shown in Table 5.

In general, the execution times were less than 2 minutes on a 333MHz PC. As it can be seen from the results, the method achieves a perfect identification in the Experiment #1 when no noise is present. The identification deteriorates in the presence of noise, as well as if the sources and detectors are not located directly above the search area. Still the inclusions with the highest intensity and the closest ones to the surface are identified, while the deepest and the weakest are lost. This can be expected, since their influence on the cost functional is becoming comparable with the background noise in the data.

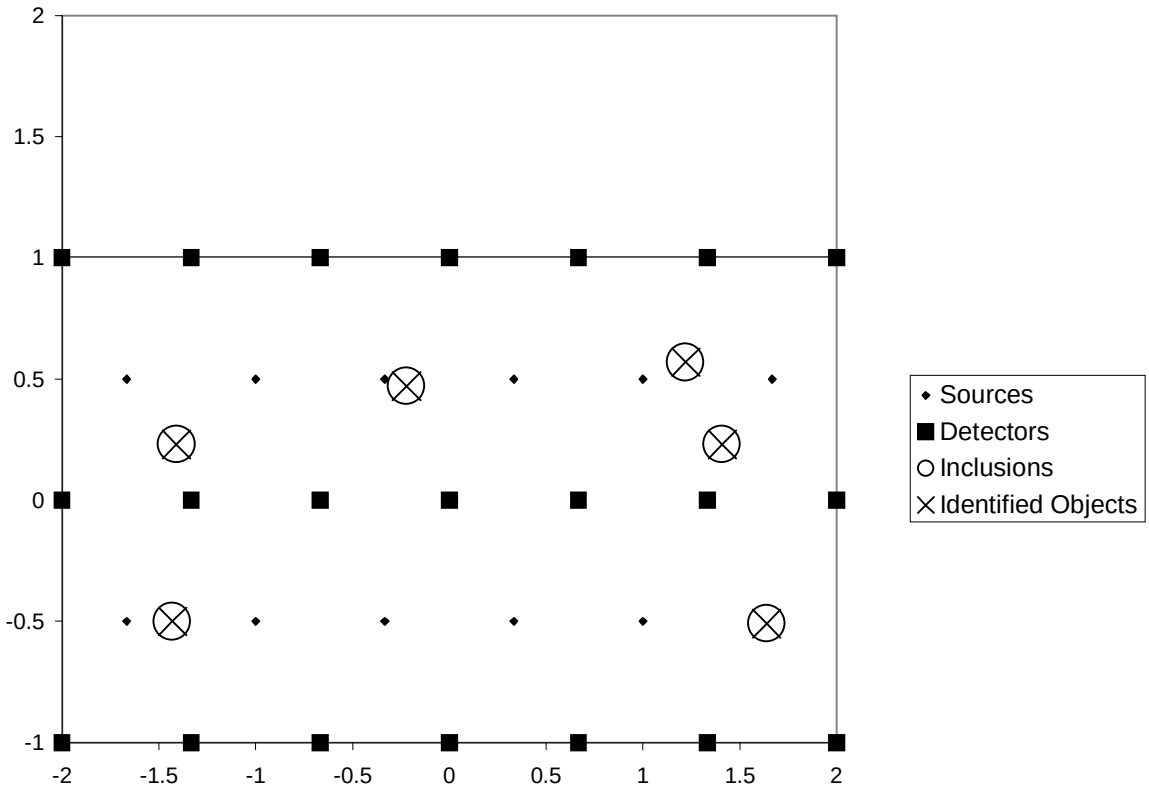

FIGURE 2. Inclusions and Identified objects for subsurface particle identification, Experiment 1, $\delta = 0.00$. x_3 coordinate is not shown.

In summary, the proposed method for the identification of small inclusions can be used in geophysics, medicine and technology. It can be useful in the development of new approaches to ultrasound mammography. It can also be used for localization of holes and cracks in metals and other materials, as well as for finding mines from surface measurements of acoustic pressure and possibly in other problems of interest in various applications.

The HSD minimization method is a specially designed low-dimensional minimization method, which is well suited for many inverse type problems. The problems do not necessarily have to be within the range of applicability of the Born approximation. It is highly desirable to apply HSD method to practical problems and to compare its performance with other methods.

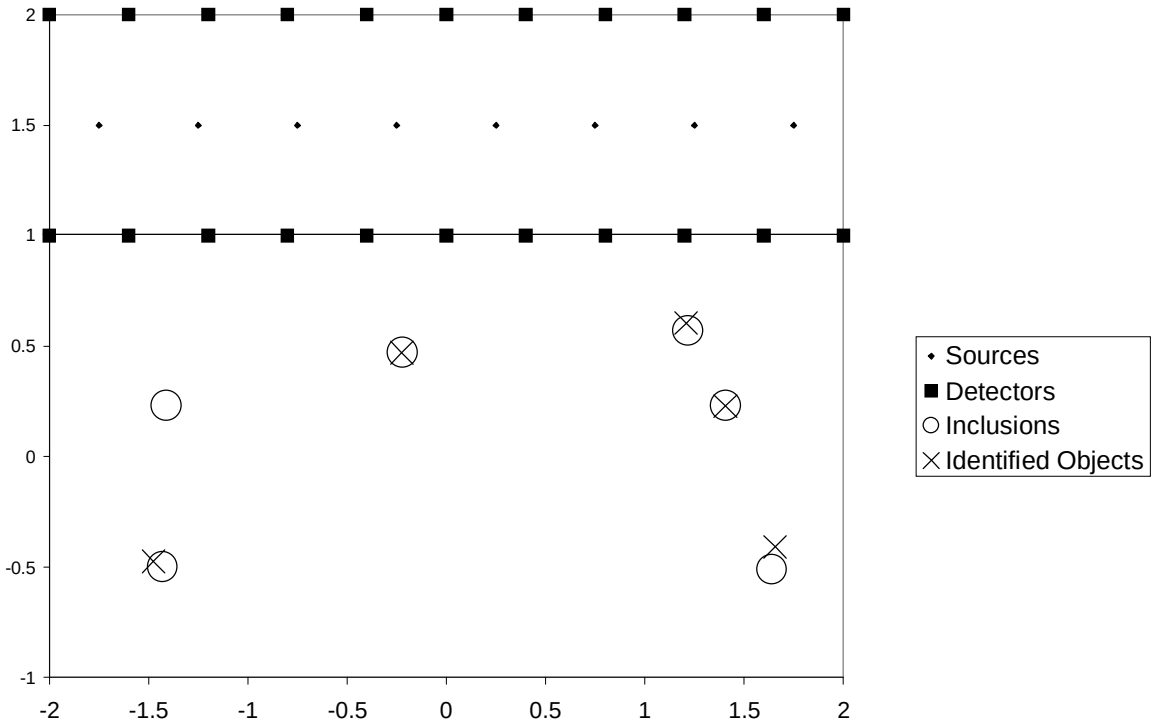

FIGURE 3. Inclusions and Identified objects for for subsurface particle identification, Experiment 2, $\delta = 0.00$. x_3 coordinate is not shown.

3. Identification of layers in multilayer particles.

3.1. Problem Description. Many practical problems require an identification of the internal structure of an object given some measurements on its surface. In this section we study such an identification for a multilayered particle illuminated by acoustic or electromagnetic plane waves. Thus the problem discussed here is an inverse scattering problem. A similar problem for the particle identification from the light scattering data is studied in [**84**]. Our approach is to reduce the inverse problem to the best fit to data multidimensional minimization.

Let $D \subset \mathbb{R}^2$ be the circle of a radius $R > 0$,

$$D_m = \{x \in \mathbb{R}^2 : r_{m-1} < |x| < r_m\,, \quad m = 1, 2, \dots, N\} \tag{3.1}$$

and $S_m = \{x \in \mathbb{R}^2 : |x| = r_m\}$ for $0 = r_0 < r_1 < \cdots < r_N < R$. Suppose that a multilayered scatterer in D has a constant refractive index n_m in the region $D_m\,, \quad m = 1, 2, \dots, N$. If the scatterer is illuminated by a plane harmonic wave then, after the time dependency is eliminated, the total field $u(x) = u_0(x) + u_s(x)$

satisfies the Helmholtz equation

$$\Delta u + k_0^2 u = 0\,, \quad |x| > r_N \tag{3.2}$$

where $u_0(x) = e^{ik_0 x\cdot\alpha}$ is the incident field and α is the unit vector in the direction of propagation. The scattered field u_s is required to satisfy the radiation condition at infinity, see [**50**].

Let $k_m^2 = k_0^2 n_m$. We consider the following transmission problem

$$\Delta u_m + k_m^2 u_m = 0 \quad x \in D_m\,, \tag{3.3}$$

under the assumption that the fields u_m and their normal derivatives are continuous across the boundaries $S_m\,,\ m = 1, 2, \ldots, N$.

In fact, the choice of the boundary conditions on the boundaries S_m depends on the physical model under the consideration. The above model may or may not be adequate for an electromagnetic or acoustic scattering, since the model may require additional parameters (such as the mass density and the compressibility) to be accounted for. However, the basic computational approach remains the same. For more details on transmission problems, including the questions on the existence and the uniqueness of the solutions, see [**3**], [**66**], and [**22**].

The Inverse Problem to be solved is:

IPS: *Given $u(x)$ for all $x \in S = \{x : |x| = R)$ at a fixed $k_0 > 0$, find the number N of the layers, the location of the layers, and their refractive indices $n_m\,,\ m = 1, 2, \ldots, N$ in* (3.3).

Here the IPS stands for a Single frequency Inverse Problem. Numerical experience shows that there are some practical difficulties in the successful resolution of the IPS even when no noise is present, see [**28**]. While there are some results on the uniqueness for the IPS (see [**3, 66**]), assuming that the refractive indices are known, and only the layers are to be identified, the stability estimates are few, [**58**],[**59**], [**68**]. The identification is successful, however, if the scatterer is subjected to a probe with plane waves of several frequencies. Thus we state the Multifrequency Inverse Problem:

IPM: *Given $u^p(x)$ for all $x \in S = \{x : |x| = R)$ at a finite number P of wave numbers $k_0^{(p)} > 0$, find the number N of the layers, the location of the layers, and their refractive indices $n_m\,,\ m = 1, 2, \ldots, N$ in* (3.3).

3.2. Best Fit Profiles and Local Minimization Methods. If the refractive indices n_m are sufficiently close to 1, then we say that the scattering is weak. In this case the scattering is described by the Born approximation, and there are methods for the solution of the above Inverse Problems. See [**15**], [**50**] and [**56**] for further details. In particular, the Born inversion is an ill-posed problem even if the Born approximation is very accurate, see [**55**], or [**53**]. When the assumption of the Born approximation is not appropriate, one matches the given observations to a set of solutions for the Direct Problem. Since our interest is in the solution of the IPS and IPM in the non-Born region of scattering, we choose to follow the best fit to data approach. This approach is used widely in a variety of applied problems, see e. g. [**7**].

Note, that, by the assumption, the scatterer has the rotational symmetry. Thus we only need to know the data for one direction of the incident plane wave. For this reason we fix $\alpha = (1, 0)$ in (3.2) and define the (complex) functions

$$g^{(p)}(\theta)\,, \quad 0 \le \theta < 2\pi, \quad p = 1, 2, \ldots, P, \tag{3.4}$$

to be the observations measured on the surface S of the ball D for a finite set of free space wave numbers $k_0^{(p)}$.

Fix a positive integer M. Given a configuration

$$Q = (r_1, r_2, \dots, r_M, n_1, n_2, \dots, n_M) \tag{3.5}$$

we solve the Direct Problem (3.2)-(3.3) (for each free space wave number $k_0^{(p)}$) with the layers $D_m = \{x \in \mathbb{R}^2 \, : r_{m-1} < |x| < r_m\,, \quad m = 1, 2, \dots, M\}$, and the corresponding refractive indices n_m, where $r_0 = 0$. Let

$$w^{(p)}(\theta) = u^{(p)}(x)\big|_{x \in S}\,. \tag{3.6}$$

Fix a set of angles $\Theta = (\theta_1, \theta_2, \dots, \theta_L)$ and let

$$\|w\|_2 = (\sum_{l=1}^{L} w^2(\theta_l))^{1/2}. \tag{3.7}$$

Define

$$\Phi(r_1, r_2, \dots, r_M, n_1, n_2, \dots, n_M) = \frac{1}{P} \sum_{p=1}^{P} \frac{\|w^{(p)} - g^{(p)}\|_2^2}{\|g^{(p)}\|_2^2}\,, \tag{3.8}$$

where the same set Θ is used for $g^{(p)}$ as for $w^{(p)}$.

We solve the IPM by minimizing the above best fit to data functional Φ over an appropriate set of admissible parameters $A_{adm} \subset \mathbb{R}^{2M}$.

It is reasonable to assume that the underlying physical problem gives some estimate for the bounds n_{low} and n_{high} of the refractive indices n_m as well as for the bound M of the expected number of layers N. Thus,

$$A_{adm} \subset \{(r_1, r_2, \dots, r_M, n_1, n_2, \dots, n_M) \;:\; 0 \le r_i \le R\,,\; n_{low} \le n_m \le n_{high}\}\,. \tag{3.9}$$

Note, that the admissible configurations must also satisfy

$$r_1 \le r_2 \le r_3 \le \cdots \le r_M\,. \tag{3.10}$$

It is well known that a multidimensional minimization is a difficult problem, unless the objective function is "well behaved". The most important quality of such a cooperative function is the presence of just a few local minima. Unfortunately, this is, decidedly, not the case in many applied problems, and, in particular, for the problem under the consideration.

To illustrate this point further, let P be the set of three free space wave numbers $k_0^{(p)}$ chosen to be

$$P = \{3.0,\ 6.5,\ 10.0\}\,. \tag{3.11}$$

Figure 4 shows the profile of the functional Φ as a function of the variable $t\,,\ 0.1 \le t \le 0.6$ in the configurations q_t with

$$n(x) = \begin{cases} 0.49 & 0 \le |x| < t \\ 9.0 & t \le |x| < 0.6 \\ 1.0 & 0.6 \le |x| \le 1.0 \end{cases}$$

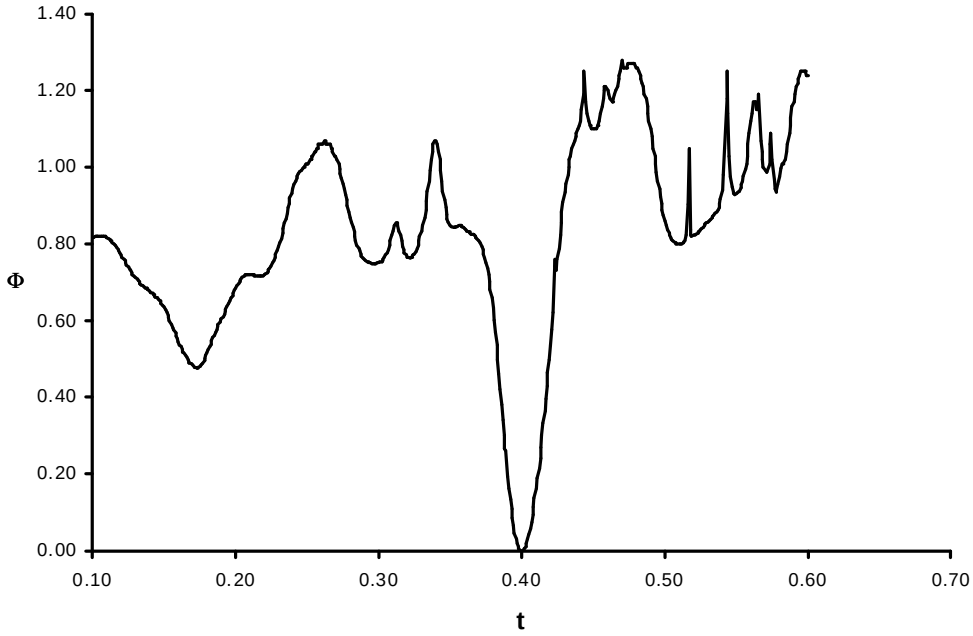

FIGURE 4. Best fit profile for the configurations q_t; Multiple frequencies $P = \{3.0,\ 6.5,\ 10.0\}$.

Thus the objective function Φ has many local minima even along this arbitrarily chosen one dimensional cross-section of the admissible set. There are sharp peaks and large gradients. Consequently, the gradient based methods (see [**11, 20, 23, 34, 38, 46**]), would not be successful for a significant portion of this region. It is also appropriate to notice that the dependency of Φ on its arguments is highly nonlinear. Thus, the gradient computations have to be done numerically, which makes them computationally expensive. More importantly, the gradient based minimization methods (as expected) perform poorly for these problems.

These complications are avoided by considering conjugate gradient type algorithms which do not require the knowledge of the derivatives at all, for example the Powell's method. Further refinements in the deterministic phase of the minimization algorithm are needed to achieve more consistent performance. They include special line minimization, and Reduction procedures similar to the ones discussed in a previous section on the identification of underground inclusions. We skip the details and refer the reader to [**28**].

In summary, the entire Local Minimization Method **(LMM)** consists of the following:

Local Minimization Method (LMM).

(1) Let your starting configuration be $Q_0 = (r_1, r_2, \ldots, r_M, n_1, n_2, \ldots, n_M)$.

(2) Apply the Reduction Procedure to Q_0, and obtain a reduced configuration Q_0^r containing M^r layers.
(3) Apply the Basic Minimization Method in $A_{adm} \bigcap \mathbb{R}^{2M^r}$ with the starting point Q_0^r, and obtain a configuration Q_1.
(4) Apply the Reduction Procedure to Q_1, and obtain a final reduced configuration Q_1^r.

3.3. Global Minimization Methods. Given an initial configuration Q_0 a local minimization method finds a local minimum near Q_0. On the other hand, global minimization methods explore the entire admissible set to find a global minimum of the objective function. While the local minimization is, usually, deterministic, the majority of the global methods are probabilistic in their nature. There is a great interest and activity in the development of efficient global minimization methods, see e.g. [**7**],[**9**]. Among them are the simulated annealing method ([**39**],[**40**]), various genetic algorithms [**33**], interval method, TRUST method ([**5**],[**6**]), etc. As we have already mentioned before, the best fit to data functional Φ has many narrow local minima. In this situation it is exceedingly unlikely to get the minima points by chance alone. Thus our special interest is for the minimization methods, which combine a global search with a local minimization. In [**27**] we developed such a method (the Hybrid Stochastic-Deterministic Method), and applied it for the identification of small subsurface particles, provided a set of surface measurements, see Sections 2.2-2.4. The HSD method could be classified as a variation of a genetic algorithm with a local search with reduction. In this paper we consider the performance of two algorithms: Deep's Method, and Rinnooy Kan and Timmer's Multilevel Single-Linkage Method. Both combine a global and a local search to determine a global minimum. Recently these methods have been applied to a similar problem of the identification of particles from their light scattering characteristics in [**84**]. Unlike [**84**], our experience shows that Deep's method has failed consistently for the type of problems we are considering. See [**19**] and [**84**] for more details on Deep's Method.

Multilevel Single-Linkage Method (MSLM). Rinnooy Kan and Timmer in [**80**] and [**81**] give a detailed description of this algorithm. Zakovic et. al. in [**84**] describe in detail an experience of its application to an inverse light scattering problem. They also discuss different stopping criteria for the MSLM. Thus, we only give here a shortened and an informal description of this method and of its algorithm.

In a pure **Random Search** method a batch H of L trial points is generated in A_{adm} using a uniformly distributed random variable. Then a local search is started from each of these L points. A local minimum with the smallest value of Φ is declared to be the global one.

A refinement of the Random Search is the **Reduced Sample Random Search** method. Here we use only a certain fixed fraction $\gamma < 1$ of the original batch of L points to proceed with the local searches. This reduced sample H_{red} of γL points is chosen to contain the points with the smallest γL values of Φ among the original batch. The local searches are started from the points in this reduced sample.

Since the local searches dominate the computational costs, we would like to initiate them only when it is truly necessary. Given a critical distance d we define

a cluster to be a group of points located within the distance d of each other. Intuitively, a local search started from the points within a cluster should result in the same local minimum, and, therefore, should be initiated only once in each cluster.

Having tried all the points in the reduced sample we have an information on the number of local searches performed and the number of local minima found. This information and the critical distance d can be used to determine a statistical level of confidence, that all the local minima have been found. The algorithm is terminated (a stopping criterion is satisfied) if an a priori level of confidence is reached.

If, however, the stopping criterion is not satisfied, we perform another iteration of the MSLM by generating another batch of L trial points. Then it is combined with the previously generated batches to obtain an enlarged batch H^j of jL points (at iteration j), which leads to a reduced sample H^j_{red} of γjL points. According to MSLM the critical distance d is reduced to d_j, (note that $d_j \to 0$ as $j \to \infty$, since we want to find a minimizer), a local minimization is attempted once within each cluster, the information on the number of local minimizations performed and the local minima found is used to determine if the algorithm should be terminated, etc.

The following is an adaptation of the MSLM method to the inverse scattering problem presented in Section 3.1. The LMM local minimization method introduced in the previous Section is used here to perform local searches.

MSLM. (at iteration j).

(1) Generate another batch of L trial points (configurations) from a random uniform distribution in A_{adm}. Combine it with the previously generated batches to obtain an enlarged batch H^j of jL points.

(2) Reduce H^j to the reduced sample H^j_{red} of γjL points, by selecting the points with the smallest γjL values of Φ in H^j.

(3) Calculate the critical distance d_j by

$$d_j^r = \pi^{-1/2} \left(\Gamma\left(1 + \frac{M}{2}\right) R^M \frac{\sigma \ln jL}{jL} \right)^{1/M},$$

$$d_j^m = \pi^{-1/2} \left(\Gamma\left(1 + \frac{M}{2}\right) (n_{high} - n_{low})^M \frac{\sigma \ln jL}{jL} \right)^{1/M}.$$

$$d_j = \sqrt{(d_j^r)^2 + (d_j^n)^2}$$

(4) Order the sample points in H^j_{red} so that $\Phi(Q_i) \le \Phi(Q_{i+1})$, $i = 1, \ldots, \gamma jL$. For each value of i, start the local minimization from Q_i, unless there exists an index $k < i$, such that $\|Q_k - Q_i\| \le d_j$. Ascertain if the result is a known local minimum.

(5) Let K be the number of local minimizations performed, and W be the number of different local minima found. Let

$$W_{tot} = \frac{W(K-1)}{K - W - 2}$$

The algorithm is terminated if

$$W_{tot} < W + 0.5\,. \tag{3.12}$$

Here Γ is the gamma function, and σ is a fixed constant.

A related algorithm (the Mode Analysis) is based on a subdivision of the admissible set into smaller volumes associated with local minima. This algorithm is also discussed in [**80**] and [**81**]. From the numerical studies presented there, the authors deduce their preference for the MSLM.

The presented MSLM algorithm was successful in the identification of various 2D layered particles, see [**28**] for details.

4. Potential scattering and the Stability Index method.

4.1. Problem description. Potential scattering problems are important in quantum mechanics, where they appear in the context of scattering of particles bombarding an atom nucleus. One is interested in reconstructing the scattering potential from the results of a scattering experiment. The examples in Section 4 deal with finding a spherically symmetric ($q = q(r),\ r = |x|$) potential from the fixed-energy scattering data, which in this case consist of the fixed-energy phase shifts. In [**60**], [**68**], [**78**] and [**79**] the three-dimensional inverse scattering problem with fixed-energy data is treated.

Let $q(x)$, $x \in \mathbb{R}^3$, be a real-valued potential with compact support. Let $R > 0$ be a number such that $q(x) = 0$ for $|x| > R$. We also assume that $q \in L^2(B_R)\,,\ B_R = \{x : |x| \leq R, x \in \mathbb{R}^3\}$. Let S^2 be the unit sphere, and $\alpha \in S^2$. For a given energy $k > 0$ the scattering solution $\psi(x, \alpha)$ is defined as the solution of

$$\Delta\psi + k^2\psi - q(x)\psi = 0\,, \quad x \in \mathbb{R}^3 \tag{4.1}$$

satisfying the following asymptotic condition at infinity:

$$\psi = \psi_0 + v, \quad \psi_0 := e^{ik\alpha\cdot x}\,, \quad \alpha \in S^2\,, \tag{4.2}$$

$$\lim_{r\to\infty} \int_{|x|=r} \left| \frac{\partial v}{\partial r} - ikv \right|^2 ds = 0\,. \tag{4.3}$$

It can be shown, that

$$\psi(x, \alpha) = \psi_0 + A(\alpha', \alpha, k)\frac{e^{ikr}}{r} + o\left(\frac{1}{r}\right)\,, \text{ as } \ r \to \infty\,, \quad \frac{x}{r} = \alpha' \quad r := |x|. \tag{4.4}$$

The function $A(\alpha', \alpha, k)$ is called the scattering amplitude, α and α' are the directions of the incident and scattered waves, and k^2 is the energy, see [**44**], [**56**].

For spherically symmetric scatterers $q(x) = q(r)$ the scattering amplitude satisfies $A(\alpha', \alpha, k) = A(\alpha' \cdot \alpha, k)$. The converse is established in [**52**]. Following [**63**], the scattering amplitude for $q = q(r)$ can be written as

$$A(\alpha', \alpha, k) = \sum_{l=0}^{\infty} \sum_{m=-l}^{l} A_l(k) Y_{lm}(\alpha') \overline{Y_{lm}(\alpha)}\,, \tag{4.5}$$

where Y_{lm} are the spherical harmonics, normalized in $L^2(S^2)$, and the bar denotes the complex conjugate.

The fixed-energy phase shifts $-\pi < \delta_l \leq \pi$ ($\delta_l = \delta(l,k)$, $k > 0$ is fixed) are related to $A_l(k)$ (see e.g., [**63**]) by the formula:

$$A_l(k) = \frac{4\pi}{k} e^{i\delta_l} \sin(\delta_l)\,. \tag{4.6}$$

Several parameter-fitting procedures were proposed for calculating the potentials from the fixed-energy phase shifts, (by Fiedledey, Lipperheide, Hooshyar and Razavy, Ioannides and Mackintosh, Newton, Sabatier, May and Scheid, Ramm and others). These works are referenced and their results are described in [**13**] and [**44**]. Recent works [**26, 28, 27, 29**] and [**67, 63, 64**], [**63**] present new numerical methods for solving this problem. In [**71**] (also see [**74, 78**]) it is proved that the R.Newton-P.Sabatier method for solving inverse scattering problem the fixed-energy phase shifts as the data (see [**44, 13**]) is fundamentally wrong in the sense that its foundation is wrong. In [**70**] a counterexample is given to a uniqueness theorem claimed in a modification of the R.Newton's inversion scheme.

Phase shifts for a spherically symmetric potential can be computed by a variety of methods, e.g. by a variable phase method described in [**12**]. The computation involves solving a nonlinear ODE for each phase shift. However, if the potential is compactly supported and piecewise-constant, then a much simpler method described in [**1**] and [**72**] can be used. We refer the reader to these papers for details.

Let $q_0(r)$ be a spherically symmetric piecewise-constant potential, $\{\tilde{\delta}(k,l)\}_{l=1}^N$ be the set of its phase shifts for a fixed $k > 0$ and a sufficiently large N. Let $q(r)$ be another potential, and let $\{\delta(k,l)\}_{l=1}^N$ be the set of its phase shifts.

The best fit to data function $\Phi(q,k)$ is defined by

$$\Phi(q,k) = \frac{\sum_{l=1}^N |\delta(k,l) - \tilde{\delta}(k,l)|^2}{\sum_{l=1}^N |\tilde{\delta}(k,l)|^2}. \tag{4.7}$$

The phase shifts are known to decay rapidly with l, see [**62**]. Thus, for sufficiently large N, the function Φ is practically the same as the one which would use all the shifts in (4.7). The inverse problem of the reconstruction of the potential from its fixed-energy phase shifts is reduced to the minimization of the objective function Φ over an appropriate admissible set.

4.2. Stability Index Minimization Method. Let the minimization problem be

$$\min\{\Phi(q) \ : \ q \in A_{adm}\} \tag{4.8}$$

Let $\tilde{q}_0$ be its global minimizer. Typically, the structure of the objective function Φ is quite complicated: this function may have many local minima. Moreover, the objective function in a neighborhood of minima can be nearly flat resulting in large minimizing sets defined by

$$S_\epsilon = \{q \in A_{adm} \ : \ \Phi(q) < \Phi(\tilde{q}_0) + \epsilon\} \tag{4.9}$$

for an $\epsilon > 0$.

Given an $\epsilon > 0$, let D_ϵ be the diameter of the minimizing set S_ϵ, which we call the **Stability Index** *D_ϵ of the minimization problem (4.8).*

Its usage is explained below.

One would expect to obtain stable identification for minimization problems with small (relative to the admissible set) stability indices. Minimization problems with large stability indices have distinct minimizers with practically the same values of the objective function. If no additional information is known, one has an uncertainty of the minimizer's choice. The stability index provides a quantitative measure of this uncertainty or instability of the minimization.

If $D_\epsilon < \eta$, where η is an a priori chosen treshold, then one can solve the global minimization problem stably. In the above general scheme it is not discussed in detail what are possible algorithms for computing the Stability Index.

One idea to construct such an algorithm is to iteratively estimate stability indices of the minimization problem, and, based on this information, to conclude if the method has achieved a stable minimum.

One such algorithm is an Iterative Reduced Random Search (IRRS) method, which uses the Stability Index for its stopping criterion. Let a batch H of L trial points be randomly generated in the admissible set A_{adm}. Let γ be a certain fixed fraction, e.g., $\gamma = 0.01$. Let S_{min} be the subset of H containing points $\{p_i\}$ with the smallest γL values of the objective function Φ in H. We call S_{min} the minimizing set. If all the minimizers in S_{min} are close to each other, then the objective function Φ is not flat near the global minimum. That is, the method identifies the minimum consistently. Let $\|\cdot\|$ be a norm in the admissible set.

Let

$$\epsilon = \max_{p_j \in S_{min}} \Phi(p_j) - \min_{p_j \in S_{min}} \Phi(p_j)$$

and

$$\tilde{D}_\epsilon = diam(S_{min}) = \max\{\|p_i - p_j\| \ : \ p_i, p_j \in S_{min}\}. \tag{4.10}$$

Then $\tilde{D}_\epsilon$ can be considered an estimate for the **Stability Index** D_ϵ of the minimization problem. The Stability Index reflects the size of the minimizing sets. Accordingly, it is used as a self-contained stopping criterion for an iterative minimization procedure. The identification is considered to be stable if the Stability Index $D_\epsilon < \eta$, for an a priori chosen $\eta > 0$. Otherwise, another batch of L trial points is generated, and the process is repeated. We used $\beta = 1.1$ as described below in the stopping criterion to determine if subsequent iterations do not produce a meaningful reduction of the objective function.

More precisely

Iterative Reduced Random Search (IRRS). (at the $j-$th iteration).
Fix $0 < \gamma < 1,\ \beta > 1,\ \eta > 0$ and N_{max}.

(1) Generate another batch H^j of L trial points in A_{adm} using a random distribution.
(2) Reduce H^j to the reduced sample H^j_{min} of γL points by selecting the points in H^j with the smallest γL values of Φ.
(3) Combine H^j_{min} with H^{j-1}_{min} obtained at the previous iteration. Let S^j_{min} be the set of γL points from $H^j_{min} \cup H^{j-1}_{min}$ with the smallest values of Φ. (Use H^1_{min} for $j = 1$).
(4) Compute the Stability Index (diameter) D^j of S^j_{min} by $D^j = \max\{\|p_i - p_k\| \ : \ p_i, p_k \in S_{min}\}$.
(5) Stopping criterion.

Let $p \in S^j_{min}$ be the point with the smallest value of Φ in S^j_{min} (the global minimizer).

If $D^j \le \eta$, then stop. The global minimizer is p. The minimization is stable.

If $D^j > \eta$ and $\Phi(q) \le \beta\Phi(p) \ : \ q \in S^j_{min}$, then stop. The minimization is unstable. The Stability Index D^j is the measure of the instability of the minimization.

Otherwise, return to step 1 and do another iteration, unless the maximum number of iterations N_{max} is exceeded.

One can make the stopping criterion more meaningful by computing a normalized stability index. This can be achieved by dividing D^j by a fixed normalization constant, such as the diameter of the entire admissible set A_{adm}. To improve the performance of the algorithm in specific problems we found it useful to modify (IRRS) by combining the stochastic (global) search with a deterministic local minimization. Such Hybrid Stochastic-Deterministic (HSD) approach has proved to be successful for a variety of problems in inverse quantum scattering (see [**72, 28, 67**]) as well as in other applications (see [**27, 26**]). A somewhat different implementation of the Stability Index Method is described in [**29**].

We seek the potentials $q(r)$ in the class of piecewise-constant, spherically symmetric real-valued functions. Let the admissible set be

(4.11)
$$A_{adm} \subset \{(r_1, r_2, \dots, r_M, q_1, q_2, \dots, q_M) \ : \ 0 \le r_i \le R\,, \ q_{low} \le q_m \le q_{high}\}\,,$$

where the bounds q_{low} and q_{high} for the potentials, as well as the bound M on the expected number of layers are assumed to be known.

A configuration $(r_1, r_2, \dots, r_M, q_1, q_2, \dots, q_M)$ corresponds to the potential

$$q(r) = q_m\,, \quad \text{for} \quad r_{m-1} \le r < r_m\,, \quad 1 \le m \le M\,, \tag{4.12}$$

where $r_0 = 0$ and $q(r) = 0$ for $r \ge r_M = R$.

Note, that the admissible configurations must also satisfy

$$r_1 \le r_2 \le r_3 \le \cdots \le r_M\,. \tag{4.13}$$

We used $\beta = 1.1$, $\epsilon = 0.02$ and $j_{max} = 30$. The choice of these and other parameters ($L = 5000$, $\gamma = 0.01$, $\nu = 0.16$) is dictated by their meaning in the algorithm and the comparative performance of the program at their different values. As usual, some adjustment of the parameters, stopping criteria, etc., is needed to achieve the optimal performance of the algorithm. The deterministic part of the IRRs algorithm was based on the Powell's minimization method, one-dimensional minimization, and a Reduction procedure similar to ones described in the previous section 3, see [**72**] for details.

4.3. Numerical Results. We studied the performance of the algorithm for 3 different potentials $q_i(r)$, $i = 1, 2, 3$ chosen from the physical considerations.

The potential $q_3(r) = -10$ for $0 \le r < 8.0$ and $q_3 = 0$ for $r \ge 8.0$ and a wave number $k = 1$ constitute a typical example for elastic scattering of neutral particles in nuclear and atomic physics. In nuclear physics one measures the length in units of fm $= 10^{-15}$m, the quantity q_3 in units of $1/\text{fm}^2$, and the wave number in units of $1/\text{fm}$. The physical potential and incident energy are given by $V(r) = \frac{\hbar^2}{2\mu} q_3(r)$ and

$E = \frac{\hbar^2 k^2}{2\mu}$, respectively. here $\hbar := \frac{h}{2\pi}$, $h = 6.62510^{-27}$ erg·s is the Planck constant, $\hbar c = 197.32$ MeV·fm, $c = 3 \cdot 10^6$ m/sec is the velocity of light, and μ is the mass of a neutron. By choosing the mass μ to be equal to the mass of a neutron $\mu =$ 939.6 MeV/c^2, the potential and energy have the values of $V(r)$ = -207.2 MeV for $0 \leq r < 8.0$ fm and $E(k =1/\text{fm}\ ) = 20.72$ MeV. In atomic physics one uses atomic units with the Bohr radius $a_0 = 0.529 \cdot 10^{-10}$m as the unit of length. Here, r, k and q_3 are measured in units of $a_0, 1/a_0$ and $1/a_0^2$, respectively. By assuming a scattering of an electron with mass $m_0 = 0.511$ MeV/c^2, we obtain the potential and energy as follows: $V(r) = -136$ eV for $0 \leq r < 8a_0 = 4.23 \cdot 10^{-10}$m and $E(k = 1/a_0) = 13.6$ eV. These numbers give motivation for the choice of examples applicable in nuclear and atomic physics.

The method used here deals with finite-range (compactly supported) potentials. One can use this method for potentials with the Coulomb tail or other potentials of interest in physics, which are not of finite range. This is done by using the phase shifts transformation method which allows one to transform the phase shifts corresponding to a potential, not of finite range, whose behavior is known for $r > a$, where a is some radius, into the phase shifts corresponding to a potential of finite range a (see [**2**], p.156).

In practice differential cross section is measured at various angles, and from it the fixed-energy phase shifts are calculated by a parameter-fitting procedure. Therefore, we plan in the future work to generalize the stability index method to the case when the original data are the values of the differential cross section, rather than the phase shifts.

For the physical reasons discussed above, we choose the following three potentials:

$$q_1(r) = \begin{cases} -2/3 & 0 \leq r < 8.0 \\ 0.0 & r \geq 8.0 \end{cases}$$

$$q_2(r) = \begin{cases} -4.0 & 0 \leq r < 8.0 \\ 0.0 & r \geq 8.0 \end{cases}$$

$$q_3(r) = \begin{cases} -10.0 & 0 \leq r < 8.0 \\ 0.0 & r \geq 8.0 \end{cases}$$

In each case the following values of the parameters have been used. The radius R of the support of each q_i was chosen to be $R = 10.0$. The admissible set A_{adm} (4.11) was defined with $M = 2$. The Reduced Random Search parameters: $L =$ 5000 , $\gamma = 0.01$, $\nu = 0.16$, $\epsilon = 0.02$, $\beta = 1.10$, $j_{max} = 30$. The value $\epsilon_r = 0.1$ was used in the Reduction Procedure during the local minimization phase. The initial configurations were generated using a random number generator with seeds determined by the system time. A typical run time was about 10 minutes on a 333 MHz PC, depending on the number of iterations in IRRS. The number N of the shifts used in (4.7) for the formation of the objective function $\Phi(q)$ was 31 for all the wave numbers. It can be seen that the shifts for the potential q_3 decay rapidly for $k = 1$, but they remain large for $k = 4$. The upper and lower bounds for the potentials $q_{low} = -20.0$ and $q_{high} = 0.0$ used in the definition of the admissible set A_{adm} were chosen to reflect a priori information about the potentials.

TABLE 6. Stability Indices for $q_1(r)$ identification at different noise levels h.

k	*Iteration*	$h = 0.00$	$h = 0.01$	$h = 0.10$
1.00	1	1.256985	0.592597	1.953778
	2	0.538440	0.133685	0.799142
	3	0.538253	0.007360	0.596742
	4	0.014616		0.123247
	5			0.015899
2.00	1	0.000000	0.020204	0.009607
2.50	1	0.000000	0.014553	0.046275
3.00	1	0.000000	0.000501	0.096444
4.00	1	0.000000	0.022935	0.027214

The identification was attempted with 3 different noise levels h. The levels are $h = 0.00$ (no noise), $h = 0.01$ and $h = 0.1$. More precisely, the noisy phase shifts $\delta_h(k, l)$ were obtained from the exact phase shifts $\delta(k, l)$ by the formula

$$\delta_h(k, l) = \delta(k, l)(1 + (0.5 - z) \cdot h)\,,$$

where z is the uniformly distributed on $[0, 1]$ random variable.

The distance $d(p_1(r), p_2(r))$ for potentials in step 5 of the IRRS algorithm was computed as

$$d(p_1(r), p_2(r)) = \|p_1(r) - p_2(r)\|$$

where the norm is the L_2-norm in $\mathbb{R}^3$.

The results of the identification algorithm (the Stability Indices) for different iterations of the IRRS algorithm are shown in Tables 6-8.

For example, Table 8 shows that for $k = 2.5,\ h = 0.00$ the Stability Index has reached the value 0.013621 after 2 iteration. According to the Stopping criterion for IRRS, the program has been terminated with the conclusion that the identification was stable. In this case the potential identified by the program was

$$p(r) = \begin{cases} -10.000024 & 0 \le r < 7.999994 \\ 0.0 & r \ge 7.999994 \end{cases}$$

which is very close to the original potential

$$q_3(r) = \begin{cases} -10.0 & 0 \le r < 8.0 \\ 0.0 & r \ge 8.0 \end{cases}$$

On the other hand, when the phase shifts of $q_3(r)$ were corrupted by a 10% noise ($k = 2.5,\ h = 0.10$), the program was terminated (according to the Stopping criterion) after 4 iterations with the Stability Index at 0.079241. Since the Stability Index is greater than the a priori chosen threshold of $\epsilon = 0.02$ the conclusion is that the identification is unstable. A closer look into this situation reveals that the values of the objective function $\Phi(p_i),\ p_i \in S_{min}$ (there are 8 elements in S_{min}) are between 0.0992806 and 0.100320. Since we chose $\beta = 1.1$ the values are within

TABLE 7. Stability Indices for $q_2(r)$ identification at different noise levels h.

k	*Iteration*	$h = 0.00$	$h = 0.01$	$h = 0.10$
1.00	1	0.774376	0.598471	0.108902
	2	0.773718	1.027345	0.023206
	3	0.026492	0.025593	0.023206
	4	0.020522	0.029533	0.024081
	5	0.020524	0.029533	0.024081
	6	0.000745	0.029533	
	7		0.029533	
	8		0.029533	
	9		0.029533	
	10		0.029533	
	11		0.029619	
	12		0.025816	
	13		0.025816	
	14		0.008901	
2.00	1	0.863796	0.799356	0.981239
	2	0.861842	0.799356	0.029445
	3	0.008653	0.000993	0.029445
	4			0.029445
	5			0.026513
	6			0.026513
	7			0.024881
2.50	1	1.848910	1.632298	0.894087
	2	1.197131	1.632298	0.507953
	3	0.580361	1.183455	0.025454
	4	0.030516	0.528979	
	5	0.016195	0.032661	
3.00	1	1.844702	1.849016	1.708201
	2	1.649700	1.782775	1.512821
	3	1.456026	1.782775	1.412345
	4	1.410253	1.457020	1.156964
	5	0.624358	0.961263	1.156964
	6	0.692080	0.961263	0.902681
	7	0.692080	0.961263	0.902681
	8	0.345804	0.291611	0.902474
	9	0.345804	0.286390	0.159221
	10	0.345804	0.260693	0.154829
	11	0.043845	0.260693	0.154829
	12	0.043845	0.260693	0.135537
	13	0.043845	0.260693	0.135537
	14	0.043845	0.260693	0.135537
	15	0.042080	0.157024	0.107548
	16	0.042080	0.157024	
	17	0.042080	0.157024	
	18	0.000429	0.157024	
	19		0.022988	
4.00	1	0.000000	0.000674	0.050705

TABLE 8. Stability Indices for $q_3(r)$ identification at different noise levels h.

k	*Iteration*	$h = 0.00$	$h = 0.01$	$h = 0.10$
1.00	1	0.564168	0.594314	0.764340
	2	0.024441	0.028558	0.081888
	3	0.024441	0.014468	0.050755
	4	0.024684		
	5	0.024684		
	6	0.005800		
2.00	1	0.684053	1.450148	0.485783
	2	0.423283	0.792431	0.078716
	3	0.006291	0.457650	0.078716
	4		0.023157	0.078716
	5			0.078716
	6			0.078716
	7			0.078716
	8			0.078716
	9			0.078716
	10			0.078716
	11			0.078716
2.50	1	0.126528	0.993192	0.996519
	2	0.013621	0.105537	0.855049
	3		0.033694	0.849123
	4		0.026811	0.079241
3.00	1	0.962483	1.541714	0.731315
	2	0.222880	0.164744	0.731315
	3	0.158809	0.021775	0.072009
	4	0.021366		
	5	0.021366		
	6	0.001416		
4.00	1	1.714951	1.413549	0.788434
	2	0.033024	0.075503	0.024482
	3	0.018250	0.029385	
	4		0.029421	
	5		0.029421	
	6		0.015946	

the required 10% of each other. The actual potentials for which the normalized distance is equal to the Stability Index 0.079241 are

$$p_1(r) = \begin{cases} -9.997164 & 0 \le r < 7.932678 \\ -7.487082 & 7.932678 \le r < 8.025500 \\ 0.0 & r \ge 8.025500 \end{cases}$$

and

$$p_2(r) = \begin{cases} -9.999565 & 0 \le r < 7.987208 \\ -1.236253 & 7.987208 \le r < 8.102628 \\ 0.0 & r \ge 8.102628 \end{cases}$$

TABLE 9. Stability Indices for $q_2(r)$ identification for different values of M.

Iteration	$M=1$	$M=2$	$M=3$	$M=4$
1	0.472661	1.068993	1.139720	1.453076
2	0.000000	0.400304	0.733490	1.453076
3		0.000426	0.125855	0.899401
4			0.125855	0.846117
5			0.033173	0.941282
6			0.033173	0.655669
7			0.033123	0.655669
8			0.000324	0.948816
9				0.025433
10				0.025433
11				0.012586

with $\Phi(p_1) = 0.0992806$ and $\Phi(p_2) = 0.0997561$. One may conclude from this example that the threshold $\epsilon = 0.02$ is too tight and can be relaxed, if the above uncertainty is acceptable.

Finally, we studied the dependency of the Stability Index from the dimension of the admissible set A_{adm}, see (4.11). This dimension is equal to $2M$, where M is the assumed number of layers in the potential. More precisely, $M = 3$, for example. means that the search is conducted in the class of potentials having 3 or less layers. The experiments were conducted for the identification of the original potential $q_2(r)$ with $k = 2.0$ and no noise present in the data. The results are shown in Table 9. Since the potential q_2 consists of only one layer, the smallest Stability Indices are obtained for $M = 1$. They gradually increase with M. Note, that the algorithm conducts the global search using random variables, so the actual values of the indices are different in every run. Still the results show the successful identification (in this case) for the entire range of the a priori chosen parameter M. This agrees with the theoretical consideration according to which the Stability Index corresponding to an ill-posed problem in an infinite-dimensional space should be large. Reducing the original ill-posed problem to a one in a space of much lower dimension regularizes the original problem.

5. Inverse scattering problem with fixed-energy data.

5.1. Problem description. In this Section we continue a discussion of the Inverse potential scattering with a presentation of Ramm's method for solving inverse scattering problem with fixed-energy data, see [**79**]. The method is applicable to both exact and noisy data. Error estimates for this method are also given. An inversion method using the Dirichlet-to-Neumann (DN) map is discussed, the difficulties of its numerical implementation are pointed out and compared with the difficulties of the implementation of the Ramm's inversion method. See the previous Section on the potential scattering for the problem set up.

5.2. Ramm's inversion method for exact data. The results we describe in this Section are taken from [**56**] and [**68**]. Assume $q \in Q := Q_a \cap L^\infty(\mathbb{R}^3)$, where $Q_a := \{q : q(x) = \overline{q(x)}, \quad q(x) \in L^2(B_a), \quad q(x) = 0 \text{ if } |x| \geq a\}$, $B_a := \{x : |x| \leq$

$a\}$. Let $A(\alpha',\alpha)$ be the corresponding scattering amplitude at a fixed energy k^2, $k=1$ is taken without loss of generality. One has:

$$A(\alpha',\alpha)=\sum_{\ell=0}^{\infty}A_\ell(\alpha)Y_\ell(\alpha'),\quad A_\ell(\alpha):=\int_{S^2}A(\alpha',\alpha)\overline{Y_\ell(\alpha')}d\alpha', \tag{5.1}$$

where S^2 is the unit sphere in $\mathbb{R}^3$, $Y_\ell(\alpha')=Y_{\ell,m}(\alpha')$, $-\ell\le m\le\ell$, are the normalized spherical harmonics, summation over m is understood in (5.1) and in (5.8) below. Define the following algebraic variety:

$$M:=\{\theta:\theta\in\mathbb{C}^3,\theta\cdot\theta=1\},\quad \theta\cdot w:=\sum_{j=1}^{3}\theta_j w_j. \tag{5.2}$$

This variety is non-compact, intersects $\mathbb{R}^3$ over S^2, and, given any $\xi\in\mathbb{R}^3$, there exist (many) $\theta,\theta'\in M$ such that

$$\theta'-\theta=\xi,\quad |\theta|\to\infty,\quad \theta,\theta'\in M. \tag{5.3}$$

In particular, if one chooses the coordinate system in which $\xi=te_3$, $t>0$, e_3 is the unit vector along the x_3-axis, then the vectors

$$\theta'=\frac{t}{2}e_3+\zeta_2e_2+\zeta_1e_1,\quad \theta=-\frac{t}{2}e_3+\zeta_2e_2+\zeta_1e_1,\quad \zeta_1^2+\zeta_2^2=1-\frac{t^2}{4}, \tag{5.4}$$

satisfy (5.3) for any complex numbers ζ_1 and ζ_2 satisfying the last equation (5.4) and such that $|\zeta_1|^2+|\zeta_2|^2\to\infty$. There are infinitely many such $\zeta_1,\zeta_2\in\mathbb{C}$. Consider a subset $M'\subset M$ consisting of the vectors $\theta=(\sin\vartheta\cos\varphi,\sin\vartheta\sin\varphi,\cos\vartheta)$, where ϑ and φ run through the whole complex plane. Clearly $\theta\in M$, but M' is a proper subset of M. Indeed, any $\theta\in M$ with $\theta_3\neq\pm1$ is an element of M'. If $\theta_3=\pm1$, then $\cos\vartheta=\pm1$, so $\sin\vartheta=0$ and one gets $\theta=(0,0,\pm1)\in M'$. However, there are vectors $\theta=(\theta_1,\theta_2,1)\in M$ which do not belong to M'. Such vectors one obtains choosing $\theta_1,\theta_2\in\mathbb{C}$ such that $\theta_1^2+\theta_2^2=0$. There are infinitely many such vectors. The same is true for vectors $(\theta_1,\theta_2,-1)$. Note that in (5.3) one can replace M by M' for any $\xi\in\mathbb{R}^3$, $\xi\neq2e_3$.

Let us state two estimates proved in [**56**]:

$$\max_{\alpha\in S^2}|A_\ell(\alpha)|\le c\left(\frac{a}{\ell}\right)^{\frac12}\left(\frac{ae}{2\ell}\right)^{\ell+1}, \tag{5.5}$$

where $c>0$ is a constant depending on the norm $||q||_{L^2(B_a)}$, and

$$|Y_\ell(\theta)|\le\frac{1}{\sqrt{4\pi}}\frac{e^{r|Im\theta|}}{|j_\ell(r)|},\quad \forall r>0,\quad \theta\in M', \tag{5.6}$$

where

$$j_\ell(r):=\left(\frac{\pi}{2r}\right)^{\frac12}J_{\ell+\frac12}(r)=\frac{1}{2\sqrt{2}}\frac{1}{\ell}\left(\frac{er}{2\ell}\right)^{\ell}[1+o(1)]\text{ as }\ell\to\infty, \tag{5.7}$$

and $J_\ell(r)$ is the Bessel function regular at $r=0$. Note that $Y_\ell(\alpha')$, defined above, admits a natural analytic continuation from S^2 to M by taking ϑ and φ to be arbitrary complex numbers. The resulting $\theta'\in M'\subset M$.

The series (5.1) converges absolutely and uniformly on the sets $S^2\times M_c$, where M_c is any compact subset of M.

Fix any numbers a_1 and b, such that $a < a_1 < b$. Let $||\cdot||$ denote the $L^2(a_1 \leq |x| \leq b)$-norm. If $|x| \geq a$, then the scattering solution is given analytically:

$$u(x,\alpha) = e^{i\alpha\cdot x} + \sum_{\ell=0}^{\infty} A_\ell(\alpha) Y_\ell(\alpha') h_\ell(r), \quad r := |x| > a, \quad \alpha' := \frac{x}{r}, \tag{5.8}$$

where $A_\ell(\alpha)$ and $Y_\ell(\alpha')$ are defined above,

$$h_\ell(r) := e^{i\frac{\pi}{2}(\ell+1)} \sqrt{\frac{\pi}{2r}} H^{(1)}_{\ell+\frac{1}{2}}(r),$$

$H^{(1)}_\ell(r)$ is the Hankel function, and the normalizing factor is chosen so that $h_\ell(r) = \frac{e^{ir}}{r}[1 + o(1)]$ as $r \to \infty$. Define

$$\rho(x) := \rho(x;\nu) := e^{-i\theta\cdot x} \int_{S^2} u(x,\alpha)\nu(\alpha,\theta)d\alpha - 1, \quad \nu \in L^2(S^2). \tag{5.9}$$

Consider the minimization problem

$$\|\rho\| = \inf := d(\theta), \tag{5.10}$$

where the infimum is taken over all $\nu \in L^2(S^2)$, and (5.3) holds.

It is proved in [**56**] that

$$d(\theta) \leq c|\theta|^{-1} \text{ if } \theta \in M, \quad |\theta| \gg 1. \tag{5.11}$$

The symbol $|\theta| \gg 1$ means that $|\theta|$ is sufficiently large. The constant $c > 0$ in (5.11) depends on the norm $\|q\|_{L^2(B_a)}$ but not on the potential $q(x)$ itself.

An algorithm for computing a function $\nu(\alpha,\theta)$, which can be used for inversion of the exact, fixed-energy, three-dimensional scattering data, is as follows:

a) Find an approximate solution to (5.10) in the sense

$$\|\rho(x,\nu)\| < 2d(\theta), \tag{5.12}$$

where in place of the factor 2 in (5.12) one could put any fixed constant greater than 1.

b) Any such $\nu(\alpha,\theta)$ generates an estimate of $\widetilde{q}(\xi)$ with the error $O\left(\frac{1}{|\theta|}\right)$, $|\theta| \to \infty$. This estimate is calculated by the formula

$$\widehat{q} := -4\pi \int_{S^2} A(\theta',\alpha)\nu(\alpha,\theta)d\alpha, \tag{5.13}$$

where $\nu(\alpha,\theta) \in L^2(S^2)$ is any function satisfying (5.12).

Our basic result is:

THEOREM 5.1. *Let* (5.3) *and* (5.12) *hold. Then*

$$\sup_{\xi\in\mathbb{R}^3} |\widehat{q} - \widetilde{q}(\xi)| \leq \frac{c}{|\theta|}, \quad |\theta| \to \infty, \tag{5.14}$$

The constant $c > 0$ in (5.14) *depends on a norm of q, but not on a particular q.*

The norm of q in the above Theorem can be any norm such that the set $\{q : ||q|| \leq const\}$ is a compact set in $L^\infty(B_a)$.

In [**56**] and [**68**] an inversion algorithm is formulated also for noisy data, and the error estimate for this algorithm is obtained. Let us describe these results.

Assume that the scattering data are given with some error: a function $A_\delta(\alpha', \alpha)$ is given such that

$$\sup_{\alpha', \alpha \in S^2} |A(\alpha', \alpha) - A_\delta(\alpha', \alpha)| \leq \delta. \tag{5.15}$$

We emphasize that $A_\delta(\alpha', \alpha)$ is not necessarily a scattering amplitude corresponding to some potential, it is an arbitrary function in $L^\infty(S^2 \times S^2)$ satisfying (5.15). It is assumed that the unknown function $A(\alpha', \alpha)$ is the scattering amplitude corresponding to a $q \in Q$.

The problem is: *Find an algorithm for calculating $\widehat{q}_\delta$ such that*

$$\sup_{\xi \in \mathbb{R}^3} |\widehat{q}_\delta - \widetilde{q}(\xi)| \leq \eta(\delta), \quad \eta(\delta) \to 0 \text{ as } \delta \to 0, \tag{5.16}$$

and estimate the rate at which $\eta(\delta)$ tends to zero.

An algorithm for inversion of noisy data will now be described.

Let

$$N(\delta) := \left[\frac{|\ln \delta|}{\ln |\ln \delta|} \right], \tag{5.17}$$

where $[x]$ is the integer nearest to $x > 0$,

$$\widehat{A}_\delta(\theta', \alpha) := \sum_{\ell=0}^{N(\delta)} A_{\delta\ell}(\alpha) Y_\ell(\theta'), \quad A_{\delta\ell}(\alpha) := \int_{S^2} A_\delta(\alpha', \alpha) \overline{Y_\ell(\alpha')} d\alpha', \tag{5.18}$$

$$u_\delta(x, \alpha) := e^{i\alpha \cdot x} + \sum_{\ell=0}^{N(\delta)} A_{\delta\ell}(\alpha) Y_\ell(\alpha') h_\ell(r), \tag{5.19}$$

$$\rho_\delta(x; \nu) := e^{-i\theta \cdot x} \int_{S^2} u_\delta(x, \alpha) \nu(\alpha) d\alpha - 1, \quad \theta \in M, \tag{5.20}$$

$$\mu(\delta) := e^{-\gamma N(\delta)}, \qquad \gamma = \ln \frac{a_1}{a} > 0, \tag{5.21}$$

$$a(\nu) := \|\nu\|_{L^2(S^2)}, \quad \kappa := |Im\theta|. \tag{5.22}$$

Consider the variational problem with constraints:

$$|\theta| = \sup := \vartheta(\delta), \tag{5.23}$$

$$|\theta| \left[\|\rho_\delta(\nu)\| + a(\nu) e^{\kappa b} \mu(\delta) \right] \leq c, \quad \theta \in M, \quad |\theta| = \sup := \vartheta(\delta), \tag{5.24}$$

the norm is defined above (5.8), and it is assumed that (5.3) holds, where $\xi \in \mathbb{R}^3$ is an arbitrary fixed vector, $c > 0$ is a sufficiently large constant, and the supremum is taken over $\theta \in M$ and $\nu \in L^2(S^2)$ under the constraint (5.24). By c we denote various positive constants.

Given $\xi \in \mathbb{R}^3$ one can always find θ and θ' such that (5.3) holds. We prove that $\vartheta(\delta) \to \infty$, more precisely:

$$\vartheta(\delta) \geq c \frac{|\ln \delta|}{(\ln |\ln \delta|)^2}, \quad \delta \to 0. \tag{5.25}$$

Let the pair $\theta(\delta)$ and $\nu_\delta(\alpha,\theta)$ be any approximate solution to problem (5.23)-(5.24) in the sense that

$$|\theta(\delta)| \geq \frac{\vartheta(\delta)}{2}. \tag{5.26}$$

Calculate

$$\widehat{q}_\delta := -4\pi \int_{S^2} \widehat{A}_\delta(\theta',\alpha)\nu_\delta(\alpha,\theta)d\alpha. \tag{5.27}$$

THEOREM 5.2. *If* (5.3) *and* (5.26) *hold, then*

$$\sup_{\xi\in\mathbb{R}^3} |\widehat{q}_\delta - \widetilde{q}(\xi)| \leq c\frac{(\ln|\ln\delta|)^2}{|\ln\delta|} \text{ as } \delta\to 0, \tag{5.28}$$

where $c>0$ is a constant depending on a norm of q.

In [**56**] estimates (5.14) and (5.28) were formulated with the supremum taken over an arbitrary large but fixed ball of radius ξ_0. Here these estimates are improved: $\xi_0=\infty$. The key point is: the constant $c>0$ in the estimate (5.11) does not depend on θ.

Remark. In [**60**] (see also [**54**] and [**68**]) an analysis of the approach to ISP, based on the recovery of the DN (Dirichle-to-Neumann) map from the fixed-energy scattering data, is given. This approach is discussed below.

The basic numerical difficulty of the approach described in Theorems 5.1 and 5.2 comes from solving problems (5.10) for exact data, and problem (5.23)-(5.24) for noisy data. Solving (5.10) amounts to finding a global minimizer of a quadratic form of the variables c_ℓ, if one takes ν in (5.9) as a linear combination of the spherical harmonics: $\nu=\sum_{\ell=0}^L c_\ell Y_\ell(\alpha)$. If one uses the necessary condition for a minimizer of a quadratic form, that is, a linear system, then the matrix of this system is ill-conditioned for large L. This causes the main difficulty in the numerical solution of (5.10). On the other hand, there are methods for global minimization of the quadratic functionals, based on the gradient descent, which may be more efficient than using the above necessary condition.

5.3. Discussion of the inversion method which uses the DN map. In [**60**] the following inversion method is discussed:

$$\tilde{q}(\xi) = \lim_{|\theta|\to\infty} \int_S \exp(-i\theta'\cdot s)(\Lambda-\Lambda_0)\psi ds, \tag{5.29}$$

where (5.3) is assumed, Λ is the Dirichlet-to-Neumann (DN) map, ψ is found from the equation:

$$\psi(s) = \psi_0(s) - \int_S G(s-t)B\psi dt, \quad B:=\Lambda-\Lambda_0, \quad \psi_0(s):=e^{i\theta\cdot s}, \tag{5.30}$$

and G is defined by the formula:

$$G(x) = \exp(i\theta\cdot x)\frac{1}{(2\pi)^3}\int_{\mathbb{R}^3}\frac{\exp(i\xi\cdot x)d\xi}{\xi^2+2\xi\cdot\theta}. \tag{5.31}$$

The DN map is constructed from the fixed-energy scattering data $A(\alpha',\alpha)$ by the method of [**60**] (see also [**56**]).

Namely, given $A(\alpha',\alpha)$ for all $\alpha',\alpha\in S^2$, one finds Λ using the following steps.

Let $f \in H^{3/2}(S)$ be given, S is a sphere of radius a centered at the origin, f_ℓ are its Fourier coefficients in the basis of the spherical harmonics,

$$w = \sum_{l=0}^{\infty} f_l Y_l(x^0) \frac{h_l(r)}{h_l(a)}, \quad r \geq a, \quad x^0 := \frac{x}{r}, \quad r := |x|. \tag{5.32}$$

Let

$$w = \int_S g(x,s)\sigma(s)ds, \tag{5.33}$$

where σ is some function, which we find below, and g is the Green function (resolvent kernel) of the Schroedinger operator, satisfying the radiation condition at infinity. Then

$$w_N^+ = w_N^- + \sigma, \tag{5.34}$$

where N is the outer normal to S, so N is directed along the radius-vector. We require $w = f$ on S. Then w is given by (5.32) in the exterior of S, and

$$w_N^- = \sum_{l=0}^{\infty} f_l Y_l(x^0) \frac{h_l'(a)}{h_l(a)}. \tag{5.35}$$

By formulas (5.34) and (5.35), finding Λ is equivalent to finding σ. By (5.33), asymptotics of w as $r := |x| \to \infty$, $x/|x| := x^0$, is (cf [**56**], p.67):

$$w = \frac{e^{ir}}{r} \frac{u(y,-x^0)}{4\pi} + o(\frac{1}{r}), \tag{5.36}$$

where u is the scattering solution,

$$u(y,-x^0) = e^{-ix^0\cdot y} + \sum_{\ell=0}^{\infty} A_\ell(-x^0) Y_\ell(y^0) h_\ell(|y|). \tag{5.37}$$

¿From (5.32), (5.36) and (5.37) one gets an equation for finding σ ([**60**], eq. (23), see also [**56**], p. 199):

$$\frac{f_l}{h_l(a)} = \frac{1}{4\pi} \int_S ds\sigma(s) \left(u(s,-\beta), Y_l(\beta)\right)_{L^2(S^2)}, \tag{5.38}$$

which can be written as a linear system:

$$\frac{4\pi f_l}{h_l(a)} = a^2(-1)^l \sum_{l'=0}^{\infty} \sigma_{l'} [4\pi i^l j_l(a)\delta_{ll'} + A_{l'l} h_{l'}(a)], \tag{5.39}$$

for the Fourier coefficients σ_ℓ of σ. The coefficients

$$A_{l'l} := ((A(\alpha',\alpha), Y_\ell(\alpha'))_{L^2(S^2)}, Y_\ell(\alpha))_{L^2(S^2)}$$

are the Fourier coefficients of the scattering amplitude. Problems (5.38) and (5.39) are very ill-posed (see [**60**] for details).

This approach faces many difficulties:

1) The construction of the DN map from the scattering data is a very ill-posed problem,

2) The construction of the potential from the DN map is a very difficult problem numerically, because one has to solve a Fredholm-type integral equation (equation (5.30)) whose kernel contains G, defined in (5.31). This G is a tempered distribution, and it is very difficult to compute it,

3) One has to calculate a limit of an integral whose integrand grows exponentially to infinity if a factor in the integrand is not known exactly. The solution of equation (5.30) is one of the factors in the integrand. It cannot be known exactly in practice because it cannot be calculated with arbitrary accuracy even if the scattering data are known exactly. Therefore the limit in formula (5.29) cannot be calculated accurately.

No error estimates are obtained for this approach.

In contrast, in Ramm's method, there is no need to compute G, to solve equation (5.30), to calculate the DN map from the scattering data, and to compute the limit (5.29). The basic difficulty in Ramm's inversion method for exact data is to minimize the quadratic form (5.10), and for noisy data to solve optimization problem (5.23)-(5.24). The error estimates are obtained for the Ramm's method.

6. Obstacle scattering by the Modified Rayleigh Conjecture (MRC) method.

6.1. Problem description. In this section we present a novel numerical method for Direct Obstacle Scattering Problems based on the Modified Rayleigh Conjecture (MRC). The basic theoretical foundation of the method was developed in [**69**]. The MRC has the appeal of an easy implementation for obstacles of complicated geometry, e.g. having edges and corners. A special version of the MRC method was used in [**32**] to compute the scattered field for 3D obstacles. In our numerical experiments the method has shown itself to be a competitive alternative to the BIEM (boundary integral equations method), see [**30**]. Also, unlike the BIEM, one can apply the algorithm to different obstacles with very little additional effort.

We formulate the obstacle scattering problem in a 3D setting with the Dirichlet boundary condition, but the discussed method can also be used for the Neumann and Robin boundary conditions.

Consider a bounded domain $D \subset \mathbb{R}^3$, with a boundary S which is assumed to be Lipschitz continuous. Denote the exterior domain by $D' = \mathbb{R}^3 \backslash D$. Let $\alpha, \alpha' \in S^2$ be unit vectors, and S^2 be the unit sphere in $\mathbb{R}^3$.

The acoustic wave scattering problem by a soft obstacle D consists in finding the (unique) solution to the problem (6.1)-(6.2):

$$\left(\nabla^2 + k^2\right) u = 0 \text{ in } D', \quad u = 0 \text{ on } S, \tag{6.1}$$

$$u = u_0 + A(\alpha', \alpha)\frac{e^{ikr}}{r} + o\left(\frac{1}{r}\right), \quad r := |x| \to \infty, \quad \alpha' := \frac{x}{r}. \tag{6.2}$$

Here $u_0 := e^{ik\alpha \cdot x}$ is the incident field, $v := u - u_0$ is the scattered field, $A(\alpha', \alpha)$ is called the scattering amplitude, its k-dependence is not shown, $k > 0$ is the wavenumber. Denote

$$A_\ell(\alpha) := \int_{S^2} A(\alpha', \alpha)\overline{Y_\ell(\alpha')}d\alpha', \tag{6.3}$$

where $Y_\ell(\alpha)$ are the orthonormal spherical harmonics, $Y_\ell = Y_{\ell m}, -\ell \leq m \leq \ell$. Let $h_\ell(r)$ be the spherical Hankel functions, normalized so that $h_\ell(r) \sim \frac{e^{ikr}}{r}$ as $r \to +\infty$.

Informally, the Random Multi-point MRC algorithm can be described as follows.

Fix a $J > 0$. Let $x_j, j = 1, 2, ..., J$ be a batch of points randomly chosen inside the obstacle D. For $x \in D'$, let

$$\alpha' = \frac{x - x_j}{|x - x_j|}, \quad \psi_\ell(x, x_j) = Y_\ell(\alpha') h_\ell(k|x - x_j|). \tag{6.4}$$

Let $g(x) = u_0(x),\ x \in S$, and minimize the discrepancy

$$\Phi(\mathbf{c}) = \|g(x) + \sum_{j=1}^{J} \sum_{\ell=0}^{L} c_{\ell,j} \psi_\ell(x, x_j)\|_{L^2(S)}, \tag{6.5}$$

over $\mathbf{c} \in \mathbb{C}^N$, where $\mathbf{c} = \{c_{\ell,j}\}$. That is, the total field $u = g(x) + v$ is desired to be as close to zero as possible at the boundary S, to satisfy the required condition for the soft scattering. If the resulting residual $r^{min} = \min \Phi$ is smaller than the prescribed tolerance ϵ, than the procedure is finished, and the sought scattered field is

$$v_\epsilon(x) = \sum_{j=1}^{J} \sum_{\ell=0}^{L} c_{\ell,j} \psi_\ell(x, x_j), \quad x \in D',$$

(see Lemma 6.1 below).

If, on the other hand, the residual $r^{min} > \epsilon$, then we continue by trying to improve on the already obtained fit in (6.5). Adjust the field on the boundary by letting $g(x) := g(x) + v_\epsilon(x),\ x \in S$. Create another batch of J points randomly chosen in the interior of D, and minimize (6.5) with this new $g(x)$. Continue with the iterations until the required tolerance ϵ on the boundary S is attained, at the same time keeping the track of the changing field v_ϵ.

Note, that the minimization in (6.5) is always done over the same number of points J. However, the points x_j are sought to be different in each iteration to assure that the minimal values of Φ are decreasing in consequent iterations. Thus, computationally, the size of the minimization problem remains the same. This is the new feature of the Random multi-point MRC method, which allows it to solve scattering problems untreatable by previously developed MRC methods, see [**30**].

Here is the precise description of the algorithm.

Random Multi-point MRC.

For $x_j \in D$, and $\ell \geq 0$ functions $\psi_\ell(x, x_j)$ are defined as in (6.4).

(1) **Initialization.** Fix $\epsilon > 0,\ L \geq 0,\ J > 0,\ N_{max} > 0$. Let $n = 0$, $v_\epsilon = 0$ and $g(x) = u_0(x),\ x \in S$.

(2) **Iteration.**

(a) Let $n := n + 1$. Randomly choose J points $x_j \in D,\ j = 1, 2, \ldots, J$.

(b) Minimize

$$\Phi(\mathbf{c}) = \|g(x) + \sum_{j=1}^{J} \sum_{\ell=0}^{L} c_{\ell,j} \psi_\ell(x, x_j)\|_{L^2(S)}$$

over $\mathbf{c} \in \mathbb{C}^N$, where $\mathbf{c} = \{c_{\ell,j}\}$.

Let the minimal value of Φ be r^{min}.

(c) Let

$$v_\epsilon(x) := v_\epsilon(x) + \sum_{j=1}^{J}\sum_{\ell=0}^{L} c_{\ell,j}\psi_\ell(x,x_j), \quad x \in D'.$$

(3) **Stopping criterion.**
   (a) If $r^{min} \leq \epsilon$, then stop.
   (b) If $r^{min} > \epsilon$, and $n \neq N_{max}$, let

$$g(x) := g(x) + \sum_{j=1}^{J}\sum_{\ell=0}^{L} c_{\ell,j}\psi_\ell(x,x_j), \quad x \in S$$

   and repeat the iterative step (2).
   (c) If $r^{min} > \epsilon$, and $n = N_{max}$, then the procedure failed.

6.2. Direct scattering problems and the Rayleigh conjecture. Let a ball $B_R := \{x : |x| \leq R\}$ contain the obstacle D. In the region $r > R$ the solution to (6.1)-(6.2) is:

$$u(x,\alpha) = e^{ik\alpha\cdot x} + \sum_{\ell=0}^{\infty} A_\ell(\alpha)\psi_\ell, \quad \psi_\ell := Y_\ell(\alpha')h_\ell(kr), \quad r > R, \quad \alpha' = \frac{x}{r}, \tag{6.6}$$

where the sum includes the summation with respect to m, $-\ell \leq m \leq \ell$, and $A_\ell(\alpha)$ are defined in (6.3).

The Rayleigh conjecture (RC) is: the series (6.6) converges up to the boundary S (originally RC dealt with periodic structures, gratings). This conjecture is false for many obstacles, but is true for some ([**4, 43, 50**]). For example, if $n = 2$ and D is an ellipse, then the series analogous to (6.6) converges in the region $r > a$, where $2a$ is the distance between the foci of the ellipse [**4**]. In the engineering literature there are numerical algorithms, based on the Rayleigh conjecture. Our aim is to give a formulation of a *Modified Rayleigh Conjecture* (MRC) which holds for any Lipschitz obstacle and can be used in numerical solution of the direct and inverse scattering problems (see [**69**]). We discuss the Dirichlet condition but similar argument is applicable to the Neumann boundary condition, corresponding to acoustically hard obstacles.

Fix $\epsilon > 0$, an arbitrary small number.

LEMMA 6.1. *There exist* $L = L(\epsilon)$ *and* $c_\ell = c_\ell(\epsilon)$ *such that*

$$||u_0 + \sum_{\ell=0}^{L(\epsilon)} c_\ell(\epsilon)\psi_\ell||_{L^2(S)} \leq \epsilon. \tag{6.7}$$

If (6.7) and the boundary condition (6.1) hold, then

$$||v_\epsilon - v||_{L^2(S)} \leq \epsilon, \quad v_\epsilon := \sum_{\ell=0}^{L(\epsilon)} c_\ell(\epsilon)\psi_\ell. \tag{6.8}$$

LEMMA 6.2. *If (6.8) holds then*

$$|||v_\epsilon - v||| = O(\epsilon), \quad \epsilon \to 0, \tag{6.9}$$

where $|||\cdot||| := ||\cdot||_{H^m_{loc}(D')} + ||\cdot||_{L^2(D';(1+|x|)^{-\gamma})}$, $\gamma > 1$, $m > 0$ *is an arbitrary integer,* H^m *is the Sobolev space, and* v_ϵ, v *in (6.9) are functions defined in* D'.

In particular, (6.9) implies

$$||v_\epsilon - v||_{L^2(S_R)} = O(\epsilon)\,, \quad \epsilon \to 0, \tag{6.10}$$

where S_R is the sphere centered at the origin with radius R.

LEMMA 6.3. *One has:*

$$c_\ell(\epsilon) \to A_\ell(\alpha)\,, \quad \forall \ell, \quad \epsilon \to 0. \tag{6.11}$$

The Modified Rayleigh Conjecture (MRC) is formulated as a theorem, which follows from the above three lemmas:

THEOREM 6.4. *For an arbitrary small $\epsilon > 0$ there exist $L(\epsilon)$ and $c_\ell(\epsilon)$, $0 \leq \ell \leq L(\epsilon)$, such that (6.7), (6.9) and (6.11) hold.*

See [**69**] for a proof of the above statements.

The difference between RC and MRC is: (6.8) does not hold if one replaces v_ϵ by $\sum_{\ell=0}^{L} A_\ell(\alpha)\psi_\ell$, and lets $L \to \infty$ (instead of letting $\epsilon \to 0$). Indeed, the series $\sum_{\ell=0}^{\infty} A_\ell(\alpha)\psi_\ell$ diverges at some points of the boundary for many obstacles. Note also that the coefficients in (6.8) depend on ϵ, so (6.8) is *not* a partial sum of a series.

For the Neumann boundary condition one minimizes

$$\left\| \frac{\partial[u_0 + \sum_{\ell=0}^{L} c_\ell \psi_\ell]}{\partial N} \right\|_{L^2(S)}$$

with respect to c_ℓ. Analogs of Lemmas 6.1-6.3 are valid and their proofs are essentially the same.

See [**75**] for an extension of these results to scattering by periodic structures.

6.3. Numerical Experiments. In this section we desribe numerical results obtained by the Random Multi-point MRC method for 2D and 3D obstacles. We also compare the 2D results to the ones obtained by our earlier method introduced in [**30**]. The method that we used previously can be described as a Multi-point MRC. Its difference from the Random Multi-point MRC method is twofold: It is just the first iteration of the Random method, and the interior points x_j, $j = 1, 2, ..., J$ were chosen deterministically, by an *ad hoc* method according to the geometry of the obstacle D. The number of points J was limited by the size of the resulting numerical minimization problem, so the accuracy of the scattering solution (i.e. the residual r^{min}) could not be made small for many obstacles. The method was not capable of treating 3D obstacles. These limitations were removed by using the Random Multi-point MRC method. As we mentioned previously, [**30**] contains a favorable comparison of the Multi-point MRC method with the BIEM, inspite in spite of the fact that the numerical implementation of the MRC method in [**30**] is considerably less efficient than the one presented in this paper.

A numerical implementation of the Random Multi-point MRC method follows the same outline as for the Multi-point MRC, which was described in [**30**]. Of course, in a 2D case, instead of (6.4) one has

$$\psi_l(x, x_j) = H_l^{(1)}(k|x - x_j|)e^{il\theta_j},$$

where $(x - x_j)/|x - x_j| = e^{i\theta_j}$.

For a numerical implementation choose M nodes $\{t_m\}$ on the surface S of the obstacle D. After the interior points $x_j,\ j = 1, 2, ..., J$ are chosen, form N vectors

$$\mathbf{a}^{(n)} = \{\psi_l(t_m, x_j)\}_{m=1}^M,$$

$n = 1, 2, \dots, N$ of length M. Note that $N = (2L+1)J$ for a 2D case, and $N = (L+1)^2 J$ for a 3D case. It is convenient to normalize the norm in $\mathbb{R}^M$ by

$$\|\mathbf{b}\|^2 = \frac{1}{M}\sum_{m=1}^{M} |b_m|^2, \quad \mathbf{b} = (b_1, b_2, ..., b_M).$$

Then $\|u_0\| = 1$.

Now let $\mathbf{b} = \{g(t_m)\}_{m=1}^M$, in the Random Multi-point MRC (see section 1), and minimize

$$\Phi(\mathbf{c}) = \|\mathbf{b} + A\mathbf{c}\|, \tag{6.12}$$

for $\mathbf{c} \in \mathbb{C}^N$, where A is the matrix containing vectors $\mathbf{a}^{(n)},\ n = 1, 2, \dots, N$ as its columns.

We used the Singular Value Decomposition (SVD) method (see e.g. [**47**]) to minimize (6.12). Small singular values $s_n < w_{min}$ of the matrix A are used to identify and delete linearly dependent or almost linearly dependent combinations of vectors $\mathbf{a}^{(n)}$. This spectral cut-off makes the minimization process stable, see the details in [**30**].

Let r^{min} be the residual, i.e. the minimal value of $\Phi(\mathbf{c})$ attained after N_{max} iterations of the Random Multi-point MRC method (or when it is stopped). For a comparison, let r_{old}^{min} be the residual obtained in [**30**] *by an earlier method.*

We conducted 2D numerical experiments for four obstacles: two ellipses of different eccentricity, a kite, and a triangle. The M=720 nodes t_m were uniformly distributed on the interval $[0, 2\pi]$, used to parametrize the boundary S. Each case was tested for wave numbers $k = 1.0$ and $k = 5.0$. Each obstacle was subjected to incident waves corresponding to $\alpha = (1.0, 0.0)$ and $\alpha = (0.0, 1.0)$.

The results for the Random Multi-point MRC with $J = 1$ are shown in Table 10, in the last column r^{min}. In every experiment the target residual $\epsilon = 0.0001$ was obtained in under 6000 iterations, in about 2 minutes run time on a 2.8 MHz PC.

In [**30**], we conducted numerical experiments for the same four 2D obstacles by a Multi-point MRC, as described in the beginning of this section. The interior points x_j were chosen differently in each experiment. Their choice is indicated in the description of each 2D experiment. The column J shows the number of these interior points. Values $L = 5$ and $M = 720$ were used in all the experiments. These results are shown in Table 10, column r_{old}^{min}.

Thus, the Random Multi-point MRC method achieved a significant improvement over the earlier Multi-point MRC.

Experiment 2D-I. The boundary S is an ellipse described by

$$\mathbf{r}(t) = (2.0\cos t,\ \sin t), \quad 0 \le t < 2\pi\,. \tag{6.13}$$

The Multi-point MRC used $J = 4$ interior points $x_j = 0.7\mathbf{r}(\frac{\pi(j-1)}{2}),\ j = 1, \dots, 4$. Run time was 2 seconds.

Experiment 2D-II. The kite-shaped boundary S (see [**17**], Section 3.5) is described by

$$\mathbf{r}(t) = (-0.65 + \cos t + 0.65\cos 2t,\ 1.5\sin t), \quad 0 \le t < 2\pi\,. \tag{6.14}$$

TABLE 10. Normalized residuals attained in the numerical experiments for 2D obstacles, $\|\mathbf{u_0}\| = 1$.

Experiment	J	k	α	r^{min}_{old}	r^{min}
I	4	1.0	$(1.0, 0.0)$	0.000201	0.0001
	4	1.0	$(0.0, 1.0)$	0.000357	0.0001
	4	5.0	$(1.0, 0.0)$	0.001309	0.0001
	4	5.0	$(0.0, 1.0)$	0.007228	0.0001
II	16	1.0	$(1.0, 0.0)$	0.003555	0.0001
	16	1.0	$(0.0, 1.0)$	0.002169	0.0001
	16	5.0	$(1.0, 0.0)$	0.009673	0.0001
	16	5.0	$(0.0, 1.0)$	0.007291	0.0001
III	16	1.0	$(1.0, 0.0)$	0.008281	0.0001
	16	1.0	$(0.0, 1.0)$	0.007523	0.0001
	16	5.0	$(1.0, 0.0)$	0.021571	0.0001
	16	5.0	$(0.0, 1.0)$	0.024360	0.0001
IV	32	1.0	$(1.0, 0.0)$	0.006610	0.0001
	32	1.0	$(0.0, 1.0)$	0.006785	0.0001
	32	5.0	$(1.0, 0.0)$	0.034027	0.0001
	32	5.0	$(0.0, 1.0)$	0.040129	0.0001

The Multi-point MRC used $J = 16$ interior points $x_j = 0.9\mathbf{r}(\frac{\pi(j-1)}{8}),\ j = 1, \dots, 16$. Run time was 33 seconds.

Experiment 2D-III. The boundary S is the triangle with vertices $(-1.0, 0.0)$ and $(1.0, \pm 1.0)$. The Multi-point MRC used the interior points $x_j = 0.9\mathbf{r}(\frac{\pi(j-1)}{8})$, $j = 1, \dots, 16$. Run time was about 30 seconds.

Experiment 2D-IV. The boundary S is an ellipse described by

$$\mathbf{r}(t) = (0.1\cos t,\ \sin t), \quad 0 \le t < 2\pi\,. \tag{6.15}$$

The Multi-point MRC used $J = 32$ interior points $x_j = 0.95\mathbf{r}(\frac{\pi(j-1)}{16}),\ j = 1, \dots, 32$. Run time was about 140 seconds.

The 3D numerical experiments were conducted for 3 obstacles: a sphere, a cube, and an ellipsoid. We used the Random Multi-point MRC with $L = 0,\ w_{min} = 10^{-12}$, and $J = 80$. The number M of the points on the boundary S is indicated in the description of the obstacles. The scattered field for each obstacle was computed for two incoming directions $\alpha_i = (\theta, \phi),\ i = 1, 2$, where ϕ was the polar angle. The first unit vector α_1 is denoted by (1) in Table 11, $\alpha_1 = (0.0, \pi/2)$. The second one is denoted by (2), $\alpha_2 = (\pi/2, \pi/4)$. A typical number of iterations N_{iter} and the run time on a 2.8 MHz PC are also shown in Table 11. For example, in experiment I with $k = 5.0$ it took about 700 iterations of the Random Multi-point MRC method to achieve the target residual $r^{min} = 0.001$ in 7 minutes.

Experiment 3D-I. The boundary S is the sphere of radius 1, with $M = 450$.

Experiment 3D-II. The boundary S is the surface of the cube $[-1, 1]^3$ with $M = 1350$.

Experiment 3D-III. The boundary S is the surface of the ellipsoid $x^2/16 + y^2 + z^2 = 1$ with $M = 450$.

TABLE 11. Normalized residuals attained in the numerical experiments for 3D obstacles, $\|\mathbf{u_0}\| = 1$.

Experiment	k	α_i	r^{min}	N_{iter}	run time
I	1.0		0.0002	1	1 sec
	5.0		0.001	700	7 min
II	1.0	(1)	0.001	800	16 min
	1.0	(2)	0.001	200	4 min
	5.0	(1)	0.0035	2000	40 min
	5.0	(2)	0.002	2000	40 min
III	1.0	(1)	0.001	3600	37 min
	1.0	(2)	0.001	3000	31 min
	5.0	(1)	0.0026	5000	53 min
	5.0	(2)	0.001	5000	53 min

In the last experiment the run time could be reduced by taking a smaller value for J. For example, the choice of $J = 8$ reduced the running time to about 6-10 minutes.

Numerical experiments show that the minimization results depend on the choice of such parameters as J, w_{min}, and L. They also depend on the choice of the interior points x_j. It is possible that further versions of the MRC could be made more efficient by finding a more efficient rule for their placement. Numerical experiments in [**30**] showed that the efficiency of the minimization greatly depended on the deterministic placement of the interior points, with better results obtained for these points placed sufficiently close to the boundary S of the obstacle D, but not very close to it. The current choice of a random placement of the interior points x_j reduced the variance in the obtained results, and eliminated the need to provide a justified algorithm for their placement. The random choice of these points distributes them in the entire interior of the obstacle, rather than in a subset of it.

6.4. Conclusions. For 3D obstacle Rayleigh's hypothesis (conjecture) says that the acoustic field u in the exterior of the obstacle D is given by the series convergent up to the boundary of D:

$$u(x,\alpha) = e^{ik\alpha\cdot x} + \sum_{\ell=0}^{\infty} A_\ell(\alpha)\psi_\ell, \quad \psi_\ell := Y_\ell(\alpha')h_\ell(kr), \quad \alpha' = \frac{x}{r}. \tag{6.16}$$

While this conjecture (RC) is false for many obstacles, it has been modified in [**69**] to obtain a valid representation for the solution of (6.1)-(6.2). This representation (Theorem 6.4) is called the Modified Rayleigh Conjecture (MRC), and is, in fact, not a conjecture, but a Theorem.

Can one use this approach to obtain solutions to various scattering problems? A straightforward numerical implementation of the MRC may fail, but, as we show here, it can be efficiently implemented and allows one to obtain accurate numerical solutions to obstacle scattering problems.

The Random Multi-point MRC algorithm was successfully applied to various 2D and 3D obstacle scattering problems. This algorithm is a significant improvement over previous MRC implementation described in [**30**]. The improvement is achieved by allowing the required minimizations to be done iteratively, while the

previous methods were limited by the problem size constraints. In [**30**], such MRC method was presented, and it favorably compared to the Boundary Integral Equation Method.

The Random Multi-point MRC has an additional attractive feature, that it can easily treat obstacles with complicated geometry (e.g. edges and corners). Unlike the BIEM, it is easily modified to treat different obstacle shapes.

Further research on MRC algorithms is conducted. It is hoped that the MRC in its various implementation can emerge as a valuable and efficient alternative to more established methods.

7. Support Function Method for inverse obstacle scattering problems.

7.1. Support Function Method (SFM). The Inverse Scattering Problem consists of finding the obstacle D from the Scattering Amplitude, or similarly observed data. The Support Function Method (SFM) was originally developed in a 3-D setting in [**48**], see also [**50**], pp 94-99. It is used to approximately locate the obstacle D. The method is derived using a high-frequency approximation to the scattered field for smooth, strictly convex obstacles. It turns out that this inexpensive method also provides a good localization of obstacles in the resonance region of frequencies. If the obstacle is not convex, then the SFM yields its convex hull.

One can restate the SFM in a 2-D setting as follows (see [**31**]). Let $D \subset \mathbb{R}^2$ be a smooth and strictly convex obstacle with the boundary Γ. Let $\nu(\mathbf{y})$ be the unique outward unit normal vector to Γ at $\mathbf{y} \in \Gamma$. Fix an incident direction $\alpha \in S^1$. Then the boundary Γ can be decomposed into the following two parts:

$$\Gamma_+ = \{\mathbf{y} \in \Gamma \ : \ \nu(\mathbf{y}) \cdot \alpha < 0\}\,, \text{ and } \quad \Gamma_- = \{\mathbf{y} \in \Gamma \ : \ \nu(\mathbf{y}) \cdot \alpha \geq 0\}\,, \tag{7.1}$$

which are, correspondingly, the illuminated and the shadowed parts of the boundary for the chosen incident direction α.

Given $\alpha \in S^1$, its **specular point** $\mathbf{s_0}(\alpha) \in \Gamma_+$ is defined from the condition:

$$\mathbf{s_0}(\alpha) \cdot \alpha = \min_{\mathbf{s} \in \Gamma_+} \mathbf{s} \cdot \alpha \tag{7.2}$$

Note that the equation of the tangent line to Γ_+ at $\mathbf{s_0}$ is

$$< x_1, x_2 > \cdot \, \alpha = \mathbf{s_0}(\alpha) \cdot \alpha\,, \tag{7.3}$$

and

$$\nu(\mathbf{s_0}(\alpha)) = -\alpha\,. \tag{7.4}$$

The **Support function** $d(\alpha)$ is defined by

$$d(\alpha) = \mathbf{s_0}(\alpha) \cdot \alpha\,. \tag{7.5}$$

Thus $|d(\alpha)|$ is the distance from the origin to the unique tangent line to Γ_+ perpendicular to the incident vector α. Since the obstacle D is assumed to be convex

$$D = \cap_{\alpha \in S^1} \{\mathbf{x} \in \mathbb{R}^2 \ : \ \mathbf{x} \cdot \alpha \geq d(\alpha)\}\,. \tag{7.6}$$

The boundary Γ of D is smooth, hence so is the Support Function. The knowledge of this function allows one to reconstruct the boundary Γ using the following procedure.

Parametrize unit vectors $\mathbf{l} \in S^1$ by $\mathbf{l}(t) = (\cos t, \sin t), \quad 0 \leq t < 2\pi$ and define

$$p(t) = d(\mathbf{l}(t)), \quad 0 \leq t < 2\pi\,. \tag{7.7}$$

Equation (7.3) and the definition of the Support Function give

$$x_1 \cos t + x_2 \sin t = p(t)\,. \tag{7.8}$$

Since Γ is the envelope of its tangent lines, its equation can be found from (7.8) and

$$-x_1 \sin t + x_2 \cos t = p'(t)\,. \tag{7.9}$$

Therefore the parametric equations of the boundary Γ are

$$x_1(t) = p(t)\cos t - p'(t)\sin t, \quad x_2(t) = p(t)\sin t + p'(t)\cos t\,. \tag{7.10}$$

So, the question is how to construct the Support function $d(\mathbf{l})$, $\mathbf{l} \in S^1$ from the knowledge of the Scattering Amplitude. In 2-D the Scattering Amplitude is related to the total field $u = u_0 + v$ by

$$A(\alpha', \alpha) = -\frac{e^{i\frac{\pi}{4}}}{\sqrt{8\pi k}} \int_\Gamma \frac{\partial u}{\partial \nu(\mathbf{y})}\; e^{-ik\alpha'\cdot\mathbf{y}}\; ds(\mathbf{y})\,. \tag{7.11}$$

In the case of the "soft" boundary condition (i.e. the pressure field satisfies the Dirichlet boundary condition $u = 0$) the Kirchhoff (high frequency) approximation gives

$$\frac{\partial u}{\partial \nu} = 2\frac{\partial u_0}{\partial \nu} \tag{7.12}$$

on the illuminated part Γ_+ of the boundary Γ, and

$$\frac{\partial u}{\partial \nu} = 0 \tag{7.13}$$

on the shadowed part Γ_-. Therefore, in this approximation,

$$A(\alpha', \alpha) = -\frac{ike^{i\frac{\pi}{4}}}{\sqrt{2\pi k}} \int_{\Gamma_+} \alpha\cdot\nu(\mathbf{y})\; e^{ik(\alpha-\alpha')\cdot\mathbf{y}}\; ds(\mathbf{y})\,. \tag{7.14}$$

Let L be the length of Γ_+, and $\mathbf{y} = \mathbf{y}(\zeta)$, $0 \le \zeta \le L$ be its arc length parametrization. Then

$$A(\alpha', \alpha) = -\frac{i\sqrt{k}\; e^{i\frac{\pi}{4}}}{\sqrt{2\pi}} \int_0^L \alpha\cdot\nu(\mathbf{y}(\zeta))\; e^{ik(\alpha-\alpha')\cdot\mathbf{y}(\zeta)}\; d\zeta\,. \tag{7.15}$$

Let $\zeta_0 \in [0, L]$ be such that $\mathbf{s}_0 = \mathbf{y}(\zeta_0)$ is the specular point of the unit vector $\mathbf{l}$, where

$$\mathbf{l} = \frac{\alpha - \alpha'}{|\alpha - \alpha'|}\,. \tag{7.16}$$

Then $\nu(\mathbf{s}_0) = -\mathbf{l}$, and $d(\mathbf{l}) = \mathbf{y}(\zeta_0)\cdot\mathbf{l}$. Let

$$\varphi(\zeta) = (\alpha - \alpha')\cdot\mathbf{y}(\zeta)\,.$$

Then $\varphi(\zeta) = \mathbf{l}\cdot\mathbf{y}(\zeta)|\alpha - \alpha'|$. Since $\nu(\mathbf{s}_0)$ and $\mathbf{y}'(\zeta_0)$ are orthogonal, one has

$$\varphi'(\zeta_0) = \mathbf{l}\cdot\mathbf{y}'(\zeta_0)|\alpha - \alpha'| = 0\,.$$

Therefore, due to the strict convexity of D, ζ_0 is also the unique non–degenerate stationary point of $\varphi(\zeta)$ on the interval $[0, L]$, that is $\varphi'(\zeta_0) = 0$, and $\varphi''(\zeta_0) \neq 0$.

According to the Stationary Phase method

(7.17)
$$\int_0^L f(\zeta)e^{ik\varphi(\zeta)}d\zeta = f(\zeta_0)\exp\left[ik\varphi(\zeta_0)+\frac{i\pi}{4}\frac{\varphi''(\zeta_0)}{|\varphi''(\zeta_0)|}\right]\sqrt{\frac{2\pi}{k|\varphi''(\zeta_0)|}}\left[1+O\left(\frac{1}{k}\right)\right],$$

as $k\to\infty$.

By the definition of the curvature $\kappa(\zeta_0)=|\mathbf{y}''(\zeta_0)|$. Therefore, from the collinearity of $\mathbf{y}''(\zeta_0)$ and $\mathbf{l}$, $|\varphi''(\zeta_0)|=|\alpha-\alpha'|\kappa(\zeta_0)$. Finally, the strict convexity of D, and the definition of $\varphi(\zeta)$, imply that ζ_0 is the unique point of minimum of φ on $[0,L]$, and

$$\frac{\varphi''(\zeta_0)}{|\varphi''(\zeta_0)|}=1\,. \tag{7.18}$$

Using (7.17)-(7.18), expression (7.15) becomes:

$$A(\alpha',\alpha)=-\frac{\mathbf{l}\cdot\alpha}{\sqrt{|\alpha-\alpha'|\kappa(\zeta_0)}}e^{ik(\alpha-\alpha')\cdot\mathbf{y}(\zeta_0)}\left[1+O\left(\frac{1}{k}\right)\right],\quad k\to\infty\,. \tag{7.19}$$

At the specular point one has $\mathbf{l}\cdot\alpha'=-\mathbf{l}\cdot\alpha$. By the definition $\alpha-\alpha'=\mathbf{l}|\alpha-\alpha'|$. Hence $\mathbf{l}\cdot(\alpha-\alpha')=|\alpha-\alpha'|$ and $2\mathbf{l}\cdot\alpha=|\alpha-\alpha'|$. These equalities and $d(\mathbf{l})=\mathbf{y}(\zeta_0)\cdot\mathbf{l}$ give

$$A(\alpha',\alpha)=-\frac{1}{2}\sqrt{\frac{|\alpha-\alpha'|}{\kappa(\zeta_0)}}e^{ik|\alpha-\alpha'|d(\mathbf{l})}\left[1+O\left(\frac{1}{k}\right)\right],\quad k\to\infty\,. \tag{7.20}$$

Thus, the approximation

$$A(\alpha',\alpha)\approx-\frac{1}{2}\sqrt{\frac{|\alpha-\alpha'|}{\kappa(\zeta_0)}}e^{ik|\alpha-\alpha'|d(\mathbf{l})} \tag{7.21}$$

can be used for an approximate recovery of the curvature and the support function (modulo $2\pi/k|\alpha-\alpha'|$) of the obstacle, provided one knows that the total field satisfies the Dirichlet boundary condition. The uncertainty in the support function determination can be remedied by using different combinations of vectors α and α' as described in the numerical results section.

Since it is also of interest to localize the obstacle in the case when the boundary condition is not a priori known, one can modify the SFM as shown in [**77**], and obtain

$$A(\alpha',\alpha)\sim\frac{1}{2}\sqrt{\frac{|\alpha-\alpha'|}{\kappa(\zeta_0)}}\;e^{i(k|\alpha-\alpha'|d(\mathbf{l})-2\gamma_0+\pi)}, \tag{7.22}$$

where

$$\gamma_0=\arctan\frac{k}{h},$$

and

$$\frac{\partial u}{\partial n}+hu=0$$

along the boundary Γ of the sought obstacle.

Now one can recover the Support Function $d(\mathbf{l})$ from (7.22), and the location of the obstacle.

7.2. Numerical results for the Support Function Method. In the first numerical experiment the obstacle is the circle

$$D = \{(x_1, x_2) \in \mathbb{R}^2 \ : \ (x_1 - 6)^2 + (x_2 - 2)^2 = 1\}. \tag{7.23}$$

It is reconstructed using the Support Function Method for two frequencies in the resonance region: $k = 1.0$, and $k = 5.0$. Table 12 shows how well the approximation (7.21) is satisfied for various pairs of vectors α and α' all representing the same vector $\mathbf{l} = (1.0, 0.0)$ according to (7.16). The Table shows the ratios of the approximate Scattering Amplitude $A_a(\alpha', \alpha)$ defined as the right hand side of the equation (7.21) to the exact Scattering Amplitude $A(\alpha', \alpha)$. Note, that for a sphere of radius a, centered at $\mathbf{x}_0 \in \mathbb{R}^2$, one has

$$A(\alpha', \alpha) = -\sqrt{\frac{2}{\pi k}}\ e^{-i\frac{\pi}{4}} e^{ik(\alpha - \alpha')\cdot \mathbf{x}_0} \sum_{l=-\infty}^{\infty} \frac{J_l(ka)}{H_l^{(1)}(ka)}\ e^{il(\theta - \beta)}, \tag{7.24}$$

where $\alpha' = \mathbf{x}/|\mathbf{x}| = e^{i\theta}$, and $\alpha = e^{i\beta}$. Vectors α and α' are defined by their polar angles shown in Table 12.

TABLE 12. Ratios of the approximate and the exact Scattering Amplitudes $A_a(\alpha', \alpha)/A(\alpha', \alpha)$ for $\mathbf{l} = (1.0, 0.0)$.

α'	α	$k = 1.0$	$k = 5.0$
π	0	0.88473 - 0.17487i	0.98859 - 0.05846i
$23\pi/24$	$\pi/24$	0.88272 - 0.17696i	0.98739 - 0.06006i
$22\pi/24$	$2\pi/24$	0.87602 - 0.18422i	0.98446 - 0.06459i
$21\pi/24$	$3\pi/24$	0.86182 - 0.19927i	0.97977 - 0.07432i
$20\pi/24$	$4\pi/24$	0.83290 - 0.22411i	0.96701 - 0.08873i
$19\pi/24$	$5\pi/24$	0.77723 - 0.25410i	0.95311 - 0.10321i
$18\pi/24$	$6\pi/24$	0.68675 - 0.27130i	0.92330 - 0.14195i
$17\pi/24$	$7\pi/24$	0.57311 - 0.25360i	0.86457 - 0.14959i
$16\pi/24$	$8\pi/24$	0.46201 - 0.19894i	0.81794 - 0.22900i
$15\pi/24$	$9\pi/24$	0.36677 - 0.12600i	0.61444 - 0.19014i
$14\pi/24$	$10\pi/24$	0.28169 - 0.05449i	0.57681 - 0.31075i
$13\pi/24$	$11\pi/24$	0.19019 + 0.00075i	0.14989 - 0.09479i
$12\pi/24$	$12\pi/24$	0.00000 + 0.00000i	0.00000 + 0.00000i

Table 12 shows that only vectors α close to the vector $\mathbf{l}$ are suitable for the Scattering Amplitude approximation. This shows the practical importance of the backscattering data. Any single combination of vectors α and α' representing $\mathbf{l}$ is not sufficient to uniquely determine the Support Function $d(\mathbf{l})$ from (7.21) because of the phase uncertainty. However, one can remedy this by using more than one pair of vectors α and α' as follows.

Let $\mathbf{l} \in S^1$ be fixed. Let

$$R(\mathbf{l}) = \{\alpha \in S^1 \ : \ |\alpha \cdot \mathbf{l}| > 1/\sqrt{2}\}.$$

Define $\Psi : \mathbb{R} \to \mathbb{R}^+$ by

$$\Psi(t) = \left\| \frac{A(\alpha', \alpha)}{|A(\alpha', \alpha)|} + e^{ik|\alpha - \alpha'|t} \right\|^2_{L^2(R(\mathbf{l}))},$$

where $\alpha' = \alpha'(\alpha)$ is defined by $\mathbf{l}$ and α according to (7.16), and the integration is done over $\alpha \in R(\mathbf{l})$.

If the approximation (7.21) were exact for any $\alpha \in R(\mathbf{l})$, then the value of $\Psi(d(\mathbf{l}))$ would be zero. This justifies the use of the minimizer $t_0 \in \mathbb{R}$ of the function $\Psi(t)$ as an approximate value of the Support Function $d(\mathbf{l})$. If the Support Function is known for sufficiently many directions $\mathbf{l} \in S^1$, the obstacle can be localized using (7.6) or (7.10). The results of such a localization for $k = 1.0$ together with the original obstacle D is shown on Figure 5. For $k = 5.0$ the identified obstacle is not shown, since it is practically the same as D. The only a priori assumption on D was that it was located inside the circle of radius 20 with the center in the origin. The Support Function was computed for 16 uniformly distributed in S^1 vectors $\mathbf{l}$. The program run takes about 80 seconds on a 333 MHz PC.

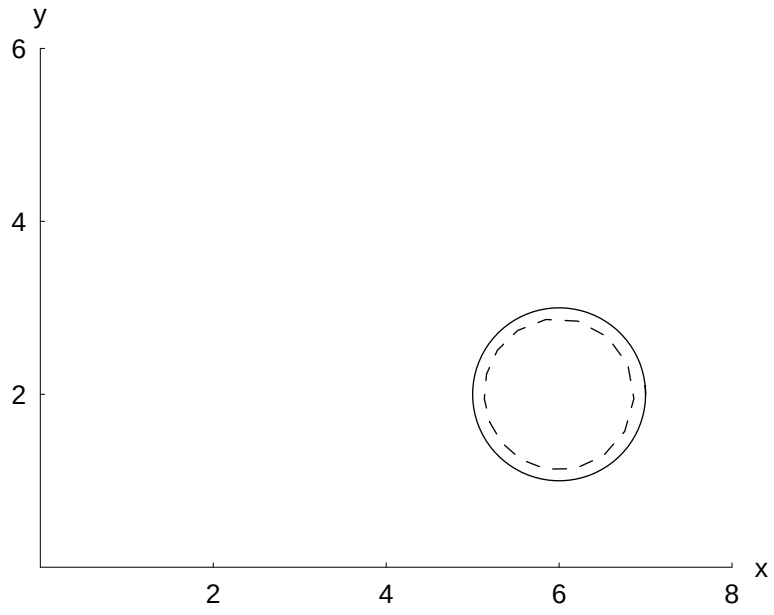

FIGURE 5. Identified (dotted line), and the original (solid line) obstacle D for $k = 1.0$.

In another numerical experiment we used $k = 1.0$ and a kite-shaped obstacle. Its boundary is described by

$$\mathbf{r}(t) = (5.35 + \cos t + 0.65 \cos 2t,\ 2.0 + 1.5 \sin t), \quad 0 \le t < 2\pi\,. \tag{7.25}$$

Numerical experiments using the boundary integral equation method (BIEM) for the direct scattering problem for this obstacle centered in the origin are described in [**17**], section 3.5. Again, the Dirichlet boundary conditions were assumed. We computed the scattering amplitude for 120 directions α using the MRC method with about 25% performance improvement over the BIEM, see [**30**].

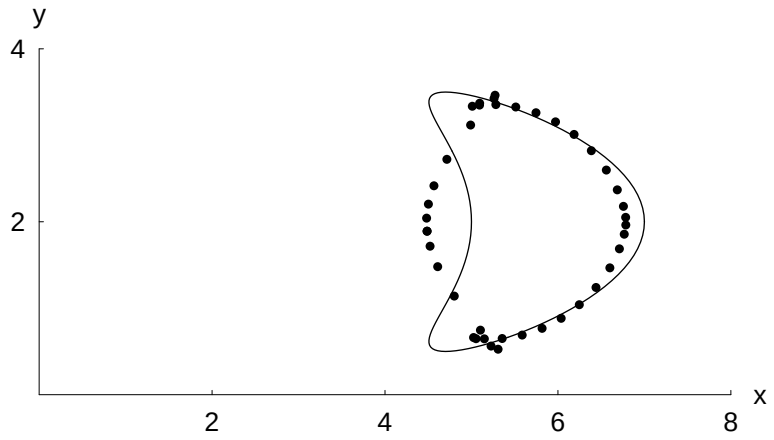

FIGURE 6. Identified points and the original obstacle D (solid line); $k = 1.0$.

The Support Function Method (SFM) was used to identify the obstacle D from the synthetic scattering amplitude with no noise added. The only a priori assumption on D was that it was located inside the circle of radius 20 with the center in the origin. The Support Function was computed for 40 uniformly distributed in S^1 vectors $\mathbf{l}$ in about 10 seconds on a 333 MHz PC. The results of the identification are shown in Figure 6. The original obstacle is the solid line. The points were identified according to (7.10). As expected, the method recovers the convex part of the boundary Γ, and fails for the concave part. The same experiment but with $k = 5.0$ achieves a perfect identification of the convex part of the boundary. In each case the convex part of the obstacle was successfully localized. Further improvements in the obstacle localization using the MRC method are suggested in [**69**], and in the next section.

For the identification of obstacles with unknown boundary conditions let

$$A(t) = A(\alpha', \alpha) = |A(t)|e^{i\psi(t)}$$

where, given t, the vectors α and α' are chosen as above, and the phase function $\psi(t)$, $\sqrt{2} < t \leq 2$ is continuous. Similarly, let $A_a(t)$, $\psi_a(t)$ be the approximate scattering amplitude and its phase defined by formula (7.22).

If the approximation (7.22) were exact for any $\alpha \in R(\mathbf{l})$, then the value of

$$|\psi_a(t) - ktd(\mathbf{l}) + 2\gamma_0 - \pi|$$

would be a multiple of 2π.

This justifies the following algorithm for the determination of the Support Function $d(\mathbf{l})$:

Use a linear regression to find the approximation

$$\psi(t) \approx C_1 t + C_2$$

on the interval $\sqrt{2} < t \leq 2$. Then

$$d(\mathbf{l}) = \frac{C_1}{k}\,. \tag{7.26}$$

TABLE 13. Identified values of the Support Function for the circle of radius 1.0 at $k = 3.0$.

h	Identified $d(\mathbf{l})$	Actual $d(\mathbf{l})$
0.01	-0.9006	-1.00
0.10	-0.9191	-1.00
0.50	-1.0072	-1.00
1.00	-1.0730	-1.00
2.00	-0.9305	-1.00
5.00	-1.3479	-1.00
10.00	-1.1693	-1.00
100.00	-1.0801	-1.00

Also

$$h = -k \tan \frac{C_2}{2}\,.$$

However, the formula for h did not work well numerically. It could only determine if the boundary conditions were or were not of the Dirichlet type. Table 13 shows that the algorithm based on (7.26) was successful in the identification of the circle of radius 1.0 centered in the origin for various values of h with no a priori assumptions on the boundary conditions. For this circle the Support Function $d(\mathbf{l}) = -1.0$ for any direction $\mathbf{l}$.

8. Analysis of a Linear Sampling method.

During the last decade many papers were published, in which the obstacle identification methods were based on a numerical verification of the inclusion of some function $f := f(\alpha, z)$, $z \in \mathbb{R}^3$, $\alpha \in S^2$, in the range $R(B)$ of a certain operator B. Examples of such methods include [**14**], [**16**],[**42**]. However, one can show that the methods proposed in the above papers have essential difficulties, see [**76**]. Although it is true that $f \notin R(B)$ when $z \notin D$, it turns out that in any neighborhood of f there are elements from $R(B)$. Also, although $f \in R(B)$ when $z \in D$, there are elements in every neighborhood of f which do not belong to $R(B)$ even if $z \in D$. Therefore it is quite difficult to construct a stable numerical method for the identification of D based on the verification of the inclusions $f \notin R(B)$, and $f \in R(B)$. Some published numerical results were intended to show that the method based on the above idea works practically, but it is not clear how these conclusions were obtained.

Let us introduce some *notations* : $N(B)$ and $R(B)$ are, respectively, the nullspace and the range of a linear operator B, $D \in \mathbb{R}^3$ is a bounded domain (obstacle) with a smooth boundary S, $D' = \mathbb{R}^3 \setminus D$, $u_0 = e^{ik\alpha\cdot x}$, $k = const > 0$, $\alpha \in S^2$ is a unit vector, N is the unit normal to S pointing into D', $g = g(x, y, k) := g(|x - y|) := \frac{e^{ik|x-y|}}{4\pi|x-y|}$, $f := e^{-ik\alpha'\cdot z}$, where $z \in \mathbb{R}^3$ and $\alpha' \in S^2$, $\alpha' := xr^{-1}$, $r = |x|$, $u = u(x, \alpha, k)$ is the scattering solution:

$$(\Delta + k^2)u = 0 \quad in \quad D', u|_S = 0, \tag{8.1}$$

$$u = u_0 + v, \quad v = A(\alpha', \alpha, k)e^{ikr}r^{-1} + o(r^{-1}), \quad as \quad r \to \infty, \tag{8.2}$$

where $A := A(\alpha', \alpha, k)$ is called the scattering amplitude, corresponding to the obstacle D and the Dirichlet boundary condition. Let $G = G(x, y, k)$ be the resolvent kernel of the Dirichlet Laplacian in D':

$$(\Delta + k^2)G = -\delta(x - y) \quad in \quad D', G|_S = 0, \tag{8.3}$$

and G satisfies the outgoing radiation condition.

If

$$(\Delta + k^2)w = 0 \quad in \quad D', w|_S = h, \tag{8.4}$$

and w satisfies the radiation condition, then ([**50**]) one has

$$w(x) = \int_S G_N(x, s)h(s)ds, \quad w = A(\alpha', k)e^{ikr}r^{-1} + o(r^{-1}), \tag{8.5}$$

as $r \to \infty$, and $xr^{-1} = \alpha'$. We write $A(\alpha')$ for $A(\alpha', k)$, and

$$A(\alpha') := Bh := \frac{1}{4\pi}\int_S u_N(s, -\alpha')h(s)ds, \tag{8.6}$$

as follows from Ramm's lemma:

Lemma 1. ([**50**], p.46) *One has:*

$$G(x, y, k) = g(r)u(y, -\alpha', k) + o(r^{-1}), \quad as \quad r = |x| \to \infty, \quad xr^{-1} = \alpha', \tag{8.7}$$

where u is the scattering solution of (8.1)-(8.2).

One can write the scattering amplitude as:

$$A(\alpha', \alpha, k) = -\frac{1}{4\pi}\int_S u_N(s, -\alpha')e^{ik\alpha\cdot s}ds. \tag{8.8}$$

The following claim follows easily from the results in [**50**], [**55**] (cf [**42**]):

Claim: $f := e^{-ik\alpha'\cdot z} \in R(B)$ if and only if $z \in D$.

Proof: If $e^{-ik\alpha'\cdot z} = Bh$, then Lemma 1 and (12.6) imply

$$g(y, z) = \int_S G_N(s, y)hds \quad \text{for} \quad |y| > |z|\,.$$

Thus $z \in D$, because otherwise one gets a contradiction: $\lim_{y\to z} g(y, z) = \infty$ if $z \in \overline{D'}$, while $\lim_{y\to z}\int_S G_N(s, y)hds < \infty$ if $z \in \overline{D'}$. Conversely, if $z \in D$, then Green's formula yields $g(y, z) = \int_S G_N(s, y)g(s, z)ds$. Taking $|y| \to \infty$, $\frac{y}{|y|} = \alpha'$, and using Lemma 1, one gets $e^{-ik\alpha'\cdot z} = Bh$, where $h = g(s, z)$. The claim is proved. □

Consider $B : L^2(S) \to L^2(S^2)$, and $A : L^2(S^2) \to L^2(S^2)$, where B is defined in (8.6) and $Aq := \int_{S^2} A(\alpha', \alpha)q(\alpha)d\alpha$. Then one proves (see [**76**]):

Theorem 1. *The ranges $R(B)$ and $R(A)$ are dense in $L^2(S^2)$*

Remark 1. In [**14**] the 2D inverse obstacle scattering problem is considered. It is proposed to solve the equation (1.9) in [**14**]:

$$\int_{S^1} A(\alpha, \beta)\mathcal{G}d\beta = e^{-ik\alpha\cdot z}, \tag{8.9}$$

where A is the scattering amplitude at a fixed $k > 0$, S^1 is the unit circle, $\alpha \in S^1$, and z is a point on $\mathbb{R}^2$. If $\mathcal{G} = \mathcal{G}(\beta, z)$ is found, the boundary S of the obstacle is to be found by finding those z for which $||\mathcal{G}|| := ||\mathcal{G}(\beta, z)||_{L^2(S^1)}$ is maximal. Assuming that k^2 is not a Dirichlet or Neumann eigenvalue of the Laplacian in D, that D is a smooth, bounded, simply connected domain, the authors state Theorem

2.1 [**14**], p.386, which says that for every $\epsilon > 0$ there exists a function $\mathcal{G} \in L^2(S^1)$, such that

$$\lim_{z \to S} ||\mathcal{G}(\beta, z)|| = \infty, \tag{8.10}$$

and (see [**14**], p.386),

$$|| \int_{S^1} A(\alpha, \beta) \mathcal{G} d\beta - e^{-ik\alpha \cdot z}|| < \epsilon. \tag{8.11}$$

There are several questions concerning the proposed method.

First, equation (8.9), in general, is not solvable. The authors propose to solve it approximately, by a regularization method. The regularization method applies for stable solution of solvable ill-posed equations (with exact or noisy data). If equation (8.9) is not solvable, it is not clear what numerical "solution" one seeks by a regularization method.

Secondly, since the kernel of the integral operator in (8.9) is smooth, one can always find, for any $z \in \mathbb{R}^2$, infinitely many $\mathcal{G}$ with arbitrary large $||\mathcal{G}||$, such that (8.11) holds. Therefore it is not clear how and why, using (8.10), one can find S numerically by the proposed method.

A numerical implementation of the Linear Sampling Method (LSM) suggested in [**14**] consists of solving a discretized version of (8.9)

$$F\mathbf{g} = \mathbf{f}, \tag{8.12}$$

where $F = \{A\alpha_i, \beta_j\}$, $i = 1, ..., N$, $j = 1, ..., N$ be a square matrix formed by the measurements of the scattering amplitude for N incoming, and N outgoing directions. In 2-D the vector $\mathbf{f}$ is formed by

$$\mathbf{f}_n = \frac{e^{i\frac{\pi}{4}}}{\sqrt{8\pi k}} e^{-ik\alpha_n \cdot z}, \quad n = 1, ..., N,$$

see [**10**] for details.

Denote the Singular Value Decomposition of the far field operator by $F = USV^H$. Let s_n be the singular values of F, $\rho = U^H\mathbf{f}$, and $\mu = V^H\mathbf{f}$. Then the norm of the sought function g is given by

$$\|\mathcal{G}\|^2 = \sum_{n=1}^{N} \frac{|\rho_n|^2}{s_n^2}. \tag{8.13}$$

A different LSM is suggested by A. Kirsch in [**42**]. In it one solves

$$(F^*F)^{1/4}\mathbf{g} = \mathbf{f} \tag{8.14}$$

instead of (8.12). The corresponding expression for the norm of $\mathcal{G}$ is

$$\|\mathcal{G}\|^2 = \sum_{n=1}^{N} \frac{|\mu_n|^2}{s_n}. \tag{8.15}$$

A detailed numerical comparison of the two LSMs and the linearized tomographic inverse scattering is given in [**10**].

The conclusions of [**10**], as well as of our own numerical experiments are that the method of Kirsch (8.14) gives a better, but a comparable identification, than (8.12). The identification is significantly deteriorating if the scattering amplitude is available only for a limited aperture, or the data are corrupted by noise. Also, the points with the *smallest* values of the $\|\mathcal{G}\|$ are the best in locating the inclusion, and

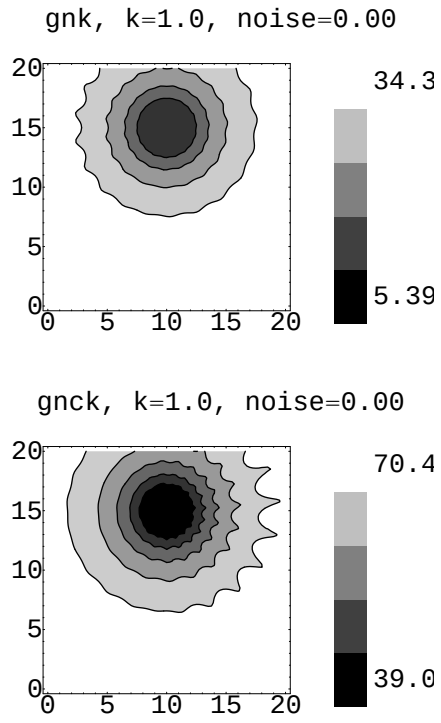

FIGURE 7. Identification of a circle at $k = 1.0$.

not the *largest* one, as required by the theory in [**42**] and in [**14**]. In Figures 7 and 8 the implementation of the Colton-Kirsch LSM (8.13) is denoted by *gnck*, and of the Kirsch method (8.15) by *gnk*. The Figures show a contour plot of the logarithm of the $\|\mathcal{G}\|$. In all the cases the original obstacle was the circle of radius 1.0 centered at the point (10.0, 15.0). A similar circular obstacle that was identified by the Support Function Method (SFM) is discussed in Section 10. Note that the actual radius of the circle is 1.0, but it cannot be seen from the LSM identification. The LSM does not require any knowledge of the boundary conditions on the obstacle. The use of the SFM for unknown boundary conditions is discussed in the previous section. The LSM identification was performed for the scattering amplitude of the circle computed analytically with no noise added. In all the experiments the value for the parameter N was chosen to be 128.

References

[1] Airapetyan, R., Ramm, A.G., Smirnova, A., [1999] *Example of two different potentials which have practically the same fixed-energy phase shifts,* Phys. Lett A, 254, N3-4, 141-148.

[2] Apagyi, B, et al (Eds) [1997] *Inverse and algebraic quantum scattering theory,* Springer, Berlin.

[3] Athanasiadis C., Ramm A.G. and Stratis I.G. [1998] *Inverse Acoustic Scattering by a Layered Obstacle,* Inverse Problems, Tomography, and Image Processing. Ramm A. ed., Plenum Press, New York, 1-8.

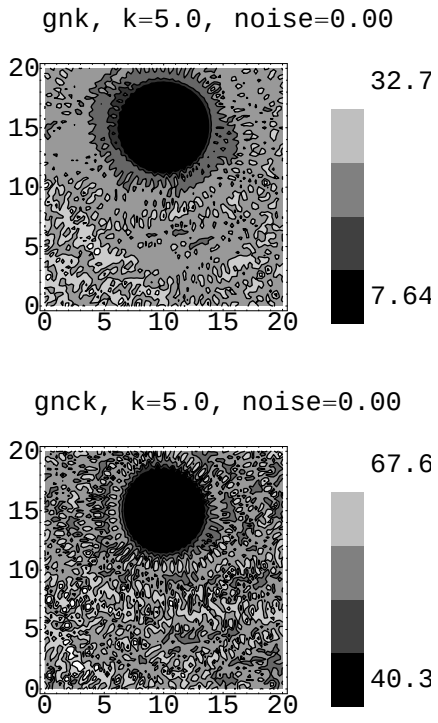

FIGURE 8. Identification of a circle at $k = 5.0$.

[4] Barantsev R, [1971] *Concerning the Rayleigh hypothesis in the problem of scattering from finite bodies of arbitrary shapes,* Vestnik Lenungrad Univ., Math., Mech., Astron., **7**, 56-62.

[5] Barhen J., Protopopescu V. [1996] *Generalized TRUST algorithm for global optimization* in State of the art in global optimization, (Floudas C., ed.), Kluwer, Dordrecht.

[6] Barhen J., Protopopescu V., Reister D. [1997] *TRUST: A deterministic algorithm for global optimization,* Science, **276**, May 16, 1094–1097.

[7] Biegler L.T. (ed.) [1997] *Large-scale optimization with applications. IMA volumes in mathematics and its applications. v.92-94,* Springer-Verlag, New York.

[8] Boender C.G.E. and Rinnooy Kan A.H.G. [1987] *Bayesian stopping rules for multistart global optimization methods,* Math. Program., **37**, 59-80.

[9] Bomze I.M. (ed.) [1997] *Developments in Global Optimization,* Kluwer Academia Publ., Dordrecht.

[10] Brandfass M., Lanterman A.D., Warnick K.F., [2001] *A comparison of the Colton-Kirsch inverse scattering methods with linearized tomographic inverse scattering,* Inverse Problems, **17**, 1797-1816.

[11] Brent P. [1973] *Algorithms for minimization without derivatives,* Prentice-Hall, Englewood Cliffs, NJ.

[12] Calogero F. [1967] *Variable Phase Approach to Potential Scattering,* Academic Press, New York and London.

[13] Chadan K., Sabatier P., [1989] *Inverse Problems in Quantum Scattering Theory,* Springer, New York.

[14] Colton, D., Kirsch, A., [1996] *A simple method for solving inverse scattering problems in the resonance region,* Inverse Problems 12, no. 4, 383–393

[15] Colton D. and Monk P. [1990] *The Inverse Scattering Problem for acoustic waves in an Inhomogeneous Medium,* Inverse problems in Partial Differential Equations. Colton D., Ewing R., Rundell W. eds., SIAM Publ. Philadelphia, 73-84.
[16] Colton, D., Coyle, J., Monk, P., [2000] *Recent developments in inverse acoustic scattering theory,* SIAM Rev. 42, no. 3, 369–414
[17] Colton D., Kress R. [1992] *Inverse Acoustic and Electromagnetic Scattering Theory,* Springer-Verlag, New York.
[18] Cox, J., Thompson, K., [1970] *Note on the uniqueness of the solution of an equation of interest in the inverse scattering problem,* J. Math. Phys., 11, N3, (1970), 815-817.
[19] Deep K. and Evans D.J. [1994] *A parallel random search global optimization method,* Technical Report 882, Computer Studies, Loughborough University of Technology.
[20] Dennis J.E. and Schnabel R.B. [1983] *Numerical methods for unconstrained optimization and nonlinear equations,* Prentice-Hall, Englewood Cliffs, NJ.
[21] Dixon L.C.W. and Jha M. [1993] *Parallel algorithms for global optimization,* J. Opt. Theor. Appl., **79**, 385-395.
[22] Ewing W.M, Jardetzky W.S and Press F. [1957] *Elastic waves in Layered Media* McGraw-Hill, New York.
[23] Fletcher R. [1981] *Practical methods of optimization v.2* John Wiley & Sons, New York.
[24] Floudas C.A. [2000] *Deterministic Global Optimization-Theory, Methods and Applications,* Vol. 37, Nonconvex Optimization and Its Applications, Kluwer Academic Publishers, Dordrecht.
[25] Floudas C.A., Pardalos P.M. [2001] *Encyclopedia of Optimization,* Kluwer Academic Publishers, Dordrecht.
[26] Gutman S. [2000] *Identification of multilayered particles from scattering data by a clustering method,* J. Comp. Phys., **163**, 529-546.
[27] Gutman S. and Ramm A.G. [2000] *Application of the Hybrid Stochastic-deterministic Minimization method to a surface data inverse scattering problem.* In the book "Operator Theory and Its Applications", Amer. Math. Soc., Fields Institute Communications, vol. **25**, pp. 293-304. (editors A.G.Ramm, P.N.Shivakumar and A.V.Strauss)
[28] Gutman S. [2001] *Identification of piecewise-constant potentials by fixed-energy shifts,* Appl. Math. Optim., **44**, 49-65.
[29] Gutman S. and Ramm A.G. [2002] *Stable identification of piecewise-constant potentials from fixed-energy phase shifts,* Jour. of Inverse and Ill-Posed Problems, 10, N4, 345-360.
[30] Gutman S., Ramm A.G. [2002] *Numerical Implementation of the MRC Method for obstacle Scattering Problems,* J. Phys. A: Math. Gen. **35**, 8065-8074.
[31] Gutman S., Ramm A.G. [2003] *Support Function Method for Inverse Scattering Problems,* In the book "Acoustics, mechanics and related topics of mathematical analysis", (ed. A.Wirgin), World Scientific, New Jersey, pp. 178-184.
[32] Gutman S., Ramm A.G. [2004] *Modified Rayleigh Conjecture method for Multidimensional Obstacle Scattering Problems,* submitted.
[33] Haupt R.L. and Haupt S.E. [1998] *Practical genetic algorithms,* John Wiley and Sons, Inc. New York.
[34] Hestenes M. [1980] *Conjugate direction methods in optimization, Applications of mathematics v.12* Springer-Verlag, New York.
[35] Horst R., Pardalos P.M., Thoai N.V. [1995] *Introduction to Global Optimization,* Kluwer Academic Publishers, Dordrecht.
[36] Horst R., Tuy H. [1993] *Global Optimization: Deterministic Approaches,* second ed., Springer, Heidelberg.
[37] Hu F.Q. [1995] *A spectral boundary integral equation method for the 2D Helholtz equation* J. Comp. Phys., **120**, 340-347.
[38] Jacobs D.A.H. (ed.) [1977] *The state of the art in numerical analysis,* Academic Press, London.
[39] Kirkpatrick S., Gelatt C.D. and Vecchi M.P. [1983] Science, **220**, 671–680.
[40] Kirkpatrick S. [1984] Journal of Statistical Physics, **34**, 975–986.
[41] Kirsch A. [1996] *An Introduction to the Mathematical Theory of Inverse Problems,* Springer-Verlag, New York.
[42] Kirsch, A., [1998] *Characterization of the shape of a scattering obstacle using the spectral data for far field operator,* Inverse Probl., 14, 1489-1512.

[43] Millar R. [1973] *The Rayleigh hypothesis and a related least-squares solution to the scattering problems for periodic surfaces and other scatterers,* Radio Sci., **8**, 785-796.
[44] Newton R., [1982] *Scattering Theory of Waves and Particles,* Springer, New York.
[45] Pardalos P.M., Romeijn H.E., Tuy H. [2000] *Recent developments and trends in global optimization,* Journal of Computational and Applied Math., 124, 209-228.
[46] Polak E. [1971] *Computational methods in optimization,* Academic Press, New York.
[47] Press W.H., Teukolsky S.A., Vetterling W.T., Flannery B.P. [1992] *Numerical Recepies in FORTRAN,* Second Ed., Cambridge University Press.
[48] Ramm A.G., [1970] *Reconstruction of the shape of a reflecting body from the scattering amplitude,* Radiofisika, 13, 727-732.
[49] Ramm A.G. [1982] *Iterative methods for calculating the static fields and wave scattering by small bodies,* Springer Verlag, New York, NY.
[50] Ramm A.G. [1986] *Scattering by Obstacles,* D. Reidel Publishing, Dordrecht, Holland.
[51] Ramm, A.G., [1988] *Recovery of the potential from fixed energy scattering data,* Inverse Problems, 4, 877-886.
[52] Ramm A.G. [1991] *Symmetry properties for scattering amplitudes and applications to inverse problems,* J. Math. Anal. Appl., **156**, 333-340.
[53] Ramm, A.G., [1990] *Is the Born approximation good for solving the inverse problem when the potential is small?* J.Math.Anal.Appl., 147, 480-485.
[54] Ramm, A.G., [1992] *Stability of the inversion of 3D fixed-frequency data,* J.Math.Anal.Appl., 169, N2, 329-349.
[55] Ramm A.G. [1992] *Multidimensional Inverse Scattering Problems,* Longman/Wiley, New York.
[56] Ramm A.G. [1994] *Multidimensional Inverse Scattering Problems,* Mir, Moscow (expanded Russian edition of [**55**].
[57] Ramm A.G., [1994] *Numerical method for solving inverse scattering problems,* Doklady of Russian Acad. of Sci., 337, N1, 20-22.
[58] Ramm A.G., [1994] *Stability of the solution to inverse obstacle scattering problem,* J.Inverse and Ill-Posed Problems, 2, N3, 269-275.
[59] Ramm A.G., [1994] *Stability estimates for obstacle scattering,* J.Math.Anal.Appl. 188, N3, 743-751.
[60] Ramm, A.G., [1996] *Finding potential from the fixed-energy scattering data via D-N map,* J. of Inverse and Ill-Posed Problems, 4, N2, 145-152.
[61] Ramm A.G. [1997] *A method for finding small inhomogeneities from surface data,* Math. Sci. Research Hot-Line, **1**, 10 , 40–42; [2000] *Finding small inhomogeneities from scattering data,* Jour. of inverse and ill-posed problems, 8, N2, 1-6.
[62] Ramm A.G., Arredondo J.H., Izquierdo B.G. [1998] *Formula for the radius of the support of the potential in terms of the scattering data,* Jour. Phys. A, **31**, N1, L39-L44.
[63] Ramm A.G., Scheid W., [1999] *An approximate method for solving inverse scattering problems with fixed-energy data,* Jour. of Inverse and Ill-posed Problems, **7**, N6, 561-571.
[64] Ramm A.G. and Smirnova A. [2000] *A numerical method for solving the inverse scattering problem with fixed-energy phase shifts,* Jour. of Inverse and Ill-Posed Problems, N3, 307-322.
[65] Ramm, A.G., [2000] *Property C for ODE and applications to inverse problems,* in the book Operator Theory and Its Applications, Amer. Math. Soc., Fields Institute Communications, Providence, RI, vol. 25, pp.15-75.
[66] Ramm A.G, Pang P., and Yan G., [2000] *A uniqueness result for the inverse transmission problem,* Internat. Jour. of Appl. Math., 2, N5, 625-634.
[67] Ramm A.G. and Gutman S. [2001] *Piecewise-constant positive potentials with practically the same fixed-energy phase shifts,* Applicable Analysis, **78**, N1-2, 207-217.
[68] Ramm, A.G., [2002] *Stability of the solutions to 3D inverse scattering problems,* Milan Journ of Math 70, 97-161.
[69] Ramm A.G. [2002] *Modified Rayleigh Conjecture and applications,* J. Phys. A: Math. Gen. **35**, L357-L361.
[70] Ramm, A.G., [2002] *A counterexample to the uniqueness result of Cox and Thompson,* Applic. Analysis, 81, N4, 833-836.
[71] Ramm A.G. [2002] *Analysis of the Newton-Sabatier scheme for inverting fixed-energy phase shifts,* Applic. Analysis, 81, N4, (2002), 965-975.

[72] Gutman S., Ramm A.G. and Scheid W. [2002] *Inverse scattering by the stability index method.* Jour. of Inverse and Ill-Posed Problems, **10**, N5, 487-502.
[73] Ramm A.G. [2004] *Dynamical systems method for solving operator equations,* Communic. in Nonlinear Science and Numer. Simulation, **9**, N2, 383-402.
[74] Ramm A.G., [2004] *One-dimensional inverse scattering and spectral problems,* Cubo a Mathem. Journ., 6, N1, 313-426.
[75] Ramm A.G., Gutman S., [2004] *Modified Rayleigh Conjecture for scattering by periodic structures,* in the book "Differential Equations and Applications", Vol. 4, (ed. Yeol Je Cho).
[76] Ramm A.G., Gutman S. *Analysis of a method for identification of obstacles,* submitted.
[77] Ramm A.G., Gutman S. [2004] *Numerical solution of obstacle scattering problems,* submitted.
[78] Ramm A.G., [2004] *Inverse Problems,* Springer, New York.
[79] Ramm A.G., [2004] *Inverse scattering with fixed-energy data,* Jour. of Indones. Math. Soc., 10, N1, (2004), 53-62.
[80] Rinnooy Kan A.H.G. and Timmer G.T. [1987] *Stochastic global optimization methods, part I: clustering methods,* Mathematical Programming, **39**, 27-56.
[81] Rinnooy Kan A.H.G. and Timmer G.T. [1987] *Stochastic global optimization methods, part II: multi level methods,* Mathematical Programming, **39**, 57-78.
[82] Rubinov, A.M., [2000] *Abstract convexity and global optimization*, Kluwer Acad. Publ., Dordrecht.
[83] Schuster G.T. [1990] *A fast exact numerical solution for the acoustic response of concentric cylinders with penetrable interfaces,* J. Acoust. Soc. Am., **87**, 495-502.
[84] Zakovic S., Ulanowski Z. and Bartholomew-Biggs M.C. [1998] *Application of global optimization to particle identification using light scattering,* Inverse Problems, **14**, 4, 1053–1067.

Department of Mathematics, Kansas State University, Manhattan, Kansas 66506-2602, USA
E-mail address: ramm@math.ksu.edu

Department of Mathematics, University of Oklahoma, Norman, OK 73019, USA
E-mail address: sgutman@ou.edu